INTERNATIONAL ATOMIC ENERGY AGENCY
UNITED NATIONS EDUCATIONAL, SCIENTIFIC AND CULTURAL ORGANIZATION
INTERNATIONAL CENTRE FOR THEORETICAL PHYSICS
I.C.T.P., P.O. BOX 586, 34100 TRIESTE, ITALY, CABLE CENTRATOM TRIESTE

H4-SMR 393/17

SPRING COLLEGE ON PLASMA PHYSICS

15 May - 9 June 1989

LASER ACCELERATORS

Francis F. Chen

Department of Electrical Engineering
University of California Los Angeles
405 Hilgard Avenue
Los Angeles 90024
U.S.A.

LASER ACCELERATORS

Francis F. Chen

PPG-1107 September, 1987

Electrical Engineering Department
University of California, Los Angeles

To be published in the Handbook of Plasma Physics, ed. by R. Z. Sagdeev and M. N. Rosenbluth, Vol. 4, "Physics of Laser Plasma," ed. by A. Rubenchik and S. Witkowski (North Holland, Amsterdam).

Chapter 4.8

Laser Accelerators

Francis F. Chen

Electrical Engineering Department, University of California
Los Angeles, California 90024, USA, (213) 825-5624

Contents

4.8.1 Introduction

As seen in other chapters in this volume, irradiation of solid targets usually results in the acceleration of electrons to high energies by plasma waves excited in parametric instabilities or resonance absorption. This chapter explores the possibility of controlling this effect to produce useful beams of high-energy particles. Of particular interest to accelerator physicists is the design of linear e^+–e^- colliders above 1 TeV. Present rf techniques have gradients of order 0.01 GeV/m, extendable to ≈ 0.1 GeV/m by semi-conventional means. TeV colliders, therefore, would be longer than 10 km. As will be seen shortly, plasma waves can have gradients of order 100 GeV/m, leading to a possible reduction of 10^3 in the length of linacs.

Though electric fields of order 1 TeV/m are readily achievable at the focus of large, pulsed lasers, laser fields in vacuum cannot be used directly for particle acceleration because a) they are transverse and oscillatory, and b) they outrun the particles, which necessarily have $v < c$. Using lasers to excite plasma waves obviates these difficulties by a) creating strong *longitudinal* fields, and b) using a plasma as a slow-wave structure which does not suffer from vacuum breakdown.

The most highly developed concept, the Beat-wave Accelerator (BWA), is directly related to stimulated Raman scattering (SRS) (Kruer and Campbell, 1988; Baldis, 1988) in that an electron plasma wave (EPW) is excited by the beat between two electromagnetic waves. In SRS, one driver (pump wave) is used,

and the EPW exponentiates unstably; in the BWA, two pump waves are used, and the EPW is driven linearly. Numerous other acceleration methods have been proposed that use laser beams and slow-wave structures other than plasmas, or use plasma waves driven by other than lasers; these can be found in a series of workshop proceedings (Channel, 1983; Bryant and Mulvey, 1984; Joshi and Katsouleas, 1985; Mills, 1987; Katsouleas, 1987; Turner, 1987). Of these, the Plasma Wake-field Accelerator (PWFA) is included here because of its similarity to the BWA.

The basic idea of the Beat-wave Accelerator is illustrated in Fig. 1. A picosecond laser beam containing two lines of the lasing medium is brought through a window into the large chamber filled with the operating gas and is focused into the plasma tube. A fully ionized, high-density plasma in the range 10^{16} - 10^{18} cm^{-3} is created by one of several possible mechanisms: θ- or z-pinch, radiofrequency waves, or multiphoton ionization. In the last case, one could use a broader, nanosecond ionizing laser beam brought in from the right, as shown. Coils for producing a confining magnetic field may be necessary. If the plasma frequency is resonant with the beat frequency of the two laser lines of the picosecond driving laser, a large-amplitude electron plasma wave is excited in the plasma. Bunches of electrons from an injector linac, shown coming from the left, enter the plasma chamber through a thin foil or a differential pumping tube and are injected into the plasma wave. The bunches are synchronized with the laser pulses. Those electrons trapped in the right phase in the wave will be accelerated by the wave's large longitudinal electric field. To increase the acceleration length, it may be necessary to trap the laser pulse by refracting it with an inverted density profile or by using relativistic self-focusing, which will be defined later. To achieve higher energy than can be gained in one stage, the modules can be repeated, with each module serving as the injector for the next. Successive modules can be optimized for the beam energy it is required to produce.

The Wake Field Accelerator has a similar, but simpler, arrangement. The injected electron beam to be accelerated to higher energy is the same, but instead of a laser, the particle beam from an existing high-energy accelerator is used to excite the plasma wave. The optical system and the frequency resonance condition are therefore eliminated. It is also possible to use lower plasma densities, in the 10^{14} - 10^{16} cm^{-3} range, at the expense of having longer acceleration lengths. This accelerator can be considered as a booster to be attached to an existing machine, allowing a fraction of the beam particles to be accelerated to much higher energy. Though basically less complicated than the Beat-wave Accelerator, the Wake Field Accelerator is more difficult to develop because a large accelerator is required for testing.

4.8.2 Beat-wave Accelerator

Fundamental relations

Two electromagnetic waves (ω_o , $\underline{k}_o$) and (ω_2 , $\underline{k}_2$) will have a beat pattern whose ponderomotive force (Chen, 1974) can excite a lower-frequency electrostatic wave (ω_1 , $\underline{k}_1$) obeying the relations

$$\omega_o = \omega_1 + \omega_2 , \quad \underline{k}_o = \underline{k}_1 + \underline{k}_2 . \tag{1}$$

If $\underline{k}_o$ and $\underline{k}_2$ are directed oppositely, $|k_1|$ is large, and the phase velocity ω_1/k_1 is too small to be useful for acceleration to GeV energies. If $\underline{k}_o$ and $\underline{k}_2$ are co-directional, fast plasma waves are excited with

$$\omega_1 = \omega_o - \omega_2 \equiv \Delta\omega \cong \omega_p \tag{2}$$

$$k_1 = k_o - k_2 \equiv \Delta k \equiv k_p . \tag{3}$$

The phase velocity $v_p \equiv \omega_1/k_1$ is seen to be equal to the group velocity of the light waves $v_g = d\omega/dk \cong \Delta\omega/\Delta k$ in the limit $\omega_p \ll \omega_o$:

$$v_p \cong v_g = c(1 - n/n_c)^{1/2} \cong c , \tag{4}$$

where

$$n/n_c \equiv \omega_p^2/\omega_o^2 , \quad \omega_p^2 \equiv 4\pi n_o e^2/m . \tag{5}$$

Defining the relativistic parameters $\beta_p \equiv v_p/c$ and $\gamma_p = (1 - \beta_p^2)^{-1/2}$, we find from Eq. (4) the convenient relation

$$\gamma_p = [1 - (1 - n/n_c)]^{-1/2} = (n_c/n)^{1/2} = \omega_o/\omega_p . \tag{6}$$

The synchronism between v_ϕ and v_g ensures that particle bunches trapped in the plasma wave will travel with the light pulse over long distances. Figure 2

shows schematically the injection and acceleration of (positive) electrons in a typical two-frequency laser pulse 10 psec (3 mm) long, containing 30 plasma wavelengths. Short pulses are necessary to avoid ion motion, which would detune the density and also permit a number of instabilities to grow.

The *cold-plasma wave-breaking limit* is found from Poisson's equation $k^2\phi = 4\pi e n_1$ when the oscillating density is set equal to the background density n_o. Thus the maximum amplitude is

$$e\phi_{max} = 4\pi n_o e^2/k_p^2 = m\omega_p^2/k_p^2 \equiv mc^2 \qquad (7)$$

for waves with relativistic v_p. Defining the relative amplitude

$$\varepsilon \equiv \phi/\phi_{max} = n_1/n_o \,, \qquad (8)$$

we find the plasma wave electric field to be

$$|E| = |k_p\phi| = \varepsilon k_p mc^2/e \equiv \varepsilon\omega_p mc/e = 0.96\,\varepsilon n^{1/2} \quad \text{V/cm} \,. \qquad (9)$$

Thus, the maximum accelerating gradient is $eE_{max} \equiv 1$ GeV/cm at $n = 10^{18}\,\text{cm}^{-3}$. The value of n_o is a compromise between large γ_p [Eq. (6)] and large E_{max} [Eq. (9)].

Beat-frequency excitation

Plasma wave excitation by optical mixing has been calculated by Rosenbluth and Liu (1972) and confirmed in computer simulations by Sullivan and Godfrey (1983), Forslund et al. (1985), and Joshi et al. (1987). The initial growth is linear at the rate

$$\partial\varepsilon/\partial t = \alpha_o\alpha_2\omega_p/4 \,, \qquad (10)$$

where

$$\alpha_j \equiv eE_j/m\omega_j c \,. \qquad (11)$$

As the oscillations grow, ω_p suffers a small redshift because of the relativistic increase in electron mass; and this detuning effect ultimately causes the waves to saturate at the level

$$\varepsilon_{sat} = (16\,\alpha_o\alpha_2/3g)^{1/3} \,, \qquad (12)$$

where the factor, $g \equiv 1 + \frac{1}{2}(\alpha_o^2 + \alpha_2^2) \equiv 1$ accounts for *transverse* electron motion in the light waves. By choosing $\Delta\omega$ to be slightly below ω_p to account for the frequency shift, Tang et al. (1985) showed that ε_{sat} can be increased to

$$\varepsilon_{sat} = 4(\alpha_o\alpha_2/3g)^{1/3} \,. \qquad (13)$$

McKinstrie and Forslund (1987) have pointed out, however, that this solution may be difficult to access in experiment, and use of Eq. (12) would be more conservative. Eqs. (12) and (13) give $\varepsilon_{sat} = 0.38$ and 0.60, respectively, for $\alpha_o = \alpha_2 = 0.1$; but effects discussed later may cause saturation at lower levels.

Eqs. (10) and (12) can be derived succinctly for $\omega_p/k_p \equiv c$. The ponderomotive force at the beat frequency is (Chen, 1974)

$$\underline{F}_{NL} = -\frac{\omega_p^2}{\omega_o\omega_2}\,\underline{\nabla}\,\frac{<2E_oE_2>}{8\pi} \,, \qquad (14)$$

where $\underline{\nabla} = i\,\underline{k}_p$. Choosing the optimum phase between E_o and E_2, discarding the non-resonant $\omega_o + \omega_2$ term, dividing by n_o, and using Eqs. (5) and (11), we find for the force on each electron

$$\underline{f}_{NL} = \tfrac{1}{2}\underline{k}_p\alpha_o\alpha_2 mc^2 \,. \qquad (15)$$

The equation of continuity is

$$\ddot{n}_1 = -\,in_o\underline{k}_p\cdot\dot{\underline{v}} \qquad (16)$$

where

$$m\dot{\underline{v}} = -\,e\,\underline{E} + \underline{f}_{NL} \qquad (17)$$

and

$$i\,\underline{k}_p\cdot\underline{E} = -\,4\pi e n_1 \,. \qquad (18)$$

Eqs. (15)-(18) yield

$$\ddot{n}_1 = -\,\omega_p^2 n_1 - \tfrac{1}{2}ik_p^2c^2n_o\alpha_o\alpha_2 \,. \qquad (19)$$

Separating the fast and slow time variations, we have $\ddot{n}_1 = (\frac{\partial}{\partial t} - i\omega_p)^2 n_1 \equiv -\,\omega_p^2 n_1 - 2i\omega_p\partial n_1/\partial t$; and the imaginary part of Eq. (19) is Eq. (10). These nonrelativistic equations can be used for the initial growth rate; but to calculate the saturation level, we must add a small relativistic correction to Eq. (17). Neglecting the driver, we have

$$\gamma\dot{\underline{v}} + \underline{v}\dot{\gamma} = -(e/m)\underline{E} \ , \quad \text{where } \gamma = (1 - v^2/c^2)^{-1/2} \ . \tag{21}$$

These give $\gamma^3\dot{\underline{v}} = -(e/m)\underline{E}$, which, together with Eqs. (16) and (18), leads to

$$\ddot{E} = -\omega_p^2 (1 - v^2/c^2)^{3/2} E \cong -\omega_p^2(1 - \frac{3}{2}\frac{v^2}{c^2})E \ . \tag{22}$$

Since $\underline{v}$ and $\underline{E}$ are out of phase, we may take $E \sim \cos \omega t$ and $v \sim \sin \omega t$. The v^2E term then is $\sim \sin^2 \omega t \cos \omega t = \cos \omega t - \cos^3 \omega t = (1/4)(\cos \omega t - \cos 3\omega t)$, of which the first term gives the nonlinear frequency shift $\delta\omega$. Since $v/c = \varepsilon$ from Eq. (16), we have

$$\omega^2 = \omega_p^2(1 - \frac{3}{2}\frac{1}{4}\varepsilon^2) \ , \quad \delta\omega = -\frac{3}{16}\omega_p\varepsilon^2(t) \ , \tag{23}$$

where $\varepsilon(t) = \alpha_o\alpha_2\omega_p t/4$ from Eq. (10). The wave stops growing when the integrated phase shift reaches 90°:

$$\frac{\pi}{2} = \int_0^t \delta\omega(t')\,dt' = (3\omega_p^3\alpha_o^2\alpha_2^2/256)\int_0^t t'^2\,dt' = \alpha_o^2\alpha_2^2(\omega_p t)^3/256 \ . \tag{24}$$

Thus,

$$\omega_p t = (128\pi/\alpha_o^2\alpha_2^2)^{1/3} \ , \tag{25}$$

$$\varepsilon_{sat} = \frac{1}{4}\alpha_o\alpha_2(128\pi/\alpha_o^2\alpha_2^2)^{1/3} = (2\pi\alpha_o\alpha_2)^{1/3} \ , \tag{26}$$

which is essentially Eq. (12).

The time τ to reach saturation, given by Eq. (25) for a square pulse, is $\tau \cong 9$ psec for $n_o = 10^{17}\,cm^{-3}$, $\alpha_o = \alpha_2 = 0.1$. Pulses longer than this would be counterproductive, giving rise to oscillations in the EPW envelope because of excessive phase slip. Inclusion of collisions leads to an asymptotic amplitude (Noble, 1985; Lee et al., 1973; Mori, 1987a), and effects of finite laser risetime have been accounted for by Forslund et al. (1985), Katsouleas et al. (1985a), and Mori (1987a).

Particle acceleration

An electron trapped at $\phi = 0$ in an EPW of amplitude εmc^2 and falling to the bottom of the potential well will gain an energy $\Delta W \cong 2\varepsilon\gamma_p^2 mc^2$. One factor of γ_p arises from Lorentz contraction of the waves, and the other from the transformation of energy back to the laboratory frame. Let a particle (β, γ) have momentum $P = \gamma\beta mc$ and energy $W = \gamma mc^2$ in the laboratory frame and quantities β', γ', p', W' in the wave frame characterized by β_p, γ_p [Eq. (6)]. The Lorentz transformation

$$\begin{pmatrix} cp \\ iW \end{pmatrix} = \begin{pmatrix} \gamma_p & -i\beta_p\gamma_p \\ i\beta_p\gamma_p & \gamma_p \end{pmatrix} \begin{pmatrix} cp' \\ iW' \end{pmatrix} \tag{27}$$

gives

$$W = \gamma_p\gamma'(1 + \beta_p\beta')\,mc^2 = \gamma mc^2 \ , \tag{28}$$

or

$$\gamma = \gamma_p\gamma'(1 + \beta_p\beta') \ . \tag{29}$$

Since $\underline{E}$ of the wave is parallel to $\underline{v}_p$, it remains invariant while $\phi = iE/k_p$ is increased by Lorentz contraction:

$$k_p' = k_p/\gamma_p \ , \quad \phi' = \gamma_p\phi \ . \tag{30}$$

In the wave frame, an electron injected at $\phi' = 0$ can gain kinetic energy $\varepsilon e\phi'_{max} = \varepsilon\gamma_p mc^2$. Its total energy W' is then $\gamma' mc^2 = (1 + \varepsilon\gamma_p)mc^2$, or

$$\gamma' = 1 + \varepsilon\gamma_p \ , \quad \beta' = [1 - (1/\gamma'^2)]^{1/2} \ . \tag{31}$$

Inserting γ' into Eq. (28) gives the energy in the laboratory, from which we must subtract the injection energy $\gamma_p mc^2$. Thus,

$$\Delta W = \gamma_p mc^2[(1 + \varepsilon\gamma_p)(1 + \beta_p\beta') - 1] \cong 2\varepsilon\gamma_p^2 mc^2 \tag{32}$$

for the usual case $\beta_p \cong \beta' \cong 1$, $\varepsilon\gamma_p \gg 1$. For instance, $\varepsilon = 0.2$ and $\gamma_p = 100$ would give $\Delta W \cong 2$ GeV. The acceleration of positrons works equally well, but heavy ions would not be interesting because, as seen in Eq. (32), the energy gain is scaled to the electron mass and would be small compared to the injection energy needed to trap the ions.

Acceleration causes the particles to slip in phase relative to the plasma wave. When the particle reaches the bottom of the potential well, it must be ejected from the system. This occurs after an acceleration length L_a given by $\Delta W / \langle eE \rangle$, where $\langle eE \rangle \cong (2/\pi)\varepsilon k_p mc^2$. Using Eq. (32) for ΔW, we find that ε cancels, and we have

$$L_a = \pi\gamma_p^2/k_p = \pi\gamma_p^2(c/\omega_o)(\omega_o/\omega_p) = \pi\gamma_p^3/k_o \ . \tag{33}$$

Thus, acceleration to large γ places stringent requirements on the production of uniform plasmas. Phase slip can be eliminated by tapering the density n_o or by using a magnetic field (Sec. 4.8.6), but staging will in any case be dictated by practical considerations. In a staged accelerator, each section of length $L \cong L_s$ has optimized n_o and γ_p and is the injector for the next section.

Injection, focusing, and beam loading

To trap a particle, a plasma wave must have amplitude $e\phi' = \gamma_p \varepsilon mc^2$ larger than the particle's kinetic energy $(\gamma' - 1)mc^2$ in the wave frame. Thus $\varepsilon > (\gamma' - 1)/\gamma_p$ is required. Transforming to the laboratory frame using the reverse of Eq. (29), we have

$$\varepsilon > \gamma(1 - \beta\beta_p) - \gamma_p^{-1} \ . \tag{34}$$

For given ε, the required injection energy is found by solving Eq. (34). In the usual case $\gamma_p \gg 1$, $\beta_p \cong 1$, the solution is approximately

$$\gamma > (1 + \varepsilon^2)/2\varepsilon \ . \tag{35}$$

This condition is, however, modified by two-dimensional effects when the injected beam has finite angular spread.

Another two-dimensional effect occurs when a plasma wave has finite width, as shown schematically in Fig. 3. Such a wave has both a longitudinal component E_z and a radial component E_r, which is 90° out of phase. Particles must be injected in the quarter cycle in which E_z is accelerating and E_r is focusing (Fedele et al., 1986). Katsouleas and Mori (Joshi et al., 1987a) have studied the trajectories of particles injected at various radii and angles, and with various energies. The trapping threshold is now a function of all these parameters, but computer simulation shows clearly the trapping, acceleration, and focusing of properly injected particles (Fig. 4).

To extract the maximum energy from the plasma waves, electron bunches injected at the right phase must also have the optimum density and shape factor. As shown by Wilks et al. (1987), injected bunches should be triangular, with the highest density at the front. This will be explained in Sec. 4.8.3.

Efficiency, cascading, and staging

The efficiency of the BWA is the product of three efficiencies: (a) conversion of electrical power into laser light, (b) conversion of laser light into plasma waves, and (c) conversion of EPW energy into that of accelerated particles.

The laser efficiency (a) has not exceeded 5% in any existing short-pulse laser; but Nd-glass, CO_2, and excimer lasers could in principle achieve 10% (Singer, 1985). Of these, only the CO_2 laser can possibly be pulsed as rapidly as 1 kHz. Higher particle-beam luminosities may require the development of free-electron lasers with MHz repetition rates and $\gtrsim 20\%$ efficiencies.

The **beam-loading** efficiency (c) is less of a problem, though a compromise must be made with energy spread. Wilks et al. (1987) showed that by proper shaping of the injected bunch, 50% is reasonable for (c). The self-magnetic field of the accelerated beam and the beam's effect on the EPW frequency are questions yet to be addressed. The beat-wave efficiency (b) is a complex question which we now discuss.

The fundamental process in beat-wave excitation is the decay of blue photons $\hbar\omega_o$ into plasmons $\hbar\omega_p$ and red photons $\hbar\omega_2$. The efficiency is limited by the Manley-Rowe relation to ω_p/ω_o. This can be augmented by **cascading**, in which $\hbar\omega_2$ decays into $\hbar\omega_p$ and a redder photon $\hbar(\omega_2 - \omega_p)$, and so on until the light pulse reaches the end of the stage or a phase mismatch develops. (The k-mismatch due to light-wave dispersion can be shown, however, to be negligible under BWA conditions.) The subsequent decays continue to feed energy into the beat wave even after the original pumps have been depleted. This gain in conversion is offset by the slightly weaker generation of higher frequency photons $\omega_n = \omega_o + n\omega_p$ in the anti-Stokes process in which a plasmon is absorbed.

Cascading of the photons and the spreading of the light-wave spectrum, first considered by Cohen et al. (1972), have been examined in the present context by Karttunen and Salomaa (1986, 1987) for finite laser risetime and electron wave damping. With dissipation, the beat-wave amplitude approaches a steady value, but for $KT_e > 100$ eV, collisions are too weak to prevent oscillation of the amplitude and sideband spectrum. Consider a square pulse just long enough to drive ε to ε_{sat} [Eq. (12)]. The pulse length L_p is approximately (Karttunen and Salomaa,

1987)

$$L_p = 8.5 / (\alpha_o\alpha_2)^{2/3} k_p \ , \qquad (36)$$

and the conversion efficiency from photons to plasmons is

$$\eta_{bw} = (L/L_p) (16\alpha_o\alpha_2/3)^{2/3} / (\alpha_o^2 + \alpha_2^2) \gamma_p^2 \ , \qquad (37)$$

where the "stage length" L is the region over which useful plasma waves exist. Eq. (37) has a broad maximum near $\alpha_o = \alpha_2$. In that symmetric case, Eqs. (36) and (37) give

$$\eta_{bw} \cong 0.18 \, k_p L \alpha_o^{2/3} / \gamma_p^2 \ . \qquad (38)$$

We may define the *depletion length* L_d to be the value of L for which $\eta_{bw} \cong 1$. We then have

$$k_p L_d \cong 5.6 \, \gamma_p^2 / \alpha_o^{2/3} \ . \qquad (39)$$

Comparing this with the acceleration length $L_a = \pi\gamma_p^2 / k_p$ [Eq. (33)], we see that

$$L_d/L_a \cong 1.8 / \alpha_o^{2/3} \ , \qquad (40)$$

which is larger than 1. It is therefore possible to make the stage length L as long as L_a without the necessity for replenishing the pump beams.

As an example, consider a stage in which $\varepsilon_{sat} = 0.2$ ($\alpha_o \cong 0.04$) and $\gamma_p^2 = 1000$ ($\Delta W = 200$ MeV, $n_o = 1.2 \times 10^{16}$ cm^{-3} for CO_2 lasers). Then $L_a = 15$ cm, $L_d/L_a \cong 16$, and $\eta_{bw} = 0.57(L/L_a) \, \alpha_o^{2/3} = 6.7\%$ for $L = L_a$, as compared with the single-step Manley-Rowe efficiency of $\omega_o/\omega_p = \gamma_p^{-1} = 3.1\%$. In a system of finite radius (Fig. 3), this result applies to the fundamental EPW mode; there may also be a small loss to the excitation of higher-order cylindrical modes.

Plasma sources

A suitable plasma for the BWA must a) have accurately controllable density n_o, b) be sufficiently long and uniform, c) not change its n_o under laser irradiation, d) keep the laser beams focused, and e) have negligible effect on the accelerated particles. In experiments in which beat-waves have been successfully excited and measured, either a fully ionized θ-pinch (Amini and Chen, 1984) or an arc-preionized, laser-heated (and fully ionized) discharge (Clayton et al., 1985)

has been used. Other experiments have documented the effectiveness of multi-photon ionization using both glass (Dangor et al., 1987) and CO_2 (Martin et al., 1987) lasers. All of these methods have satisfied (a)-(c) above with $n_o \cong 10^{17}$ cm^{-3}, $T_e = 2$–30 eV, and lengths of 2–10 mm. Future experiments requiring longer plasmas and perhaps lower densities (for the wake-field accelerator) may require development of UV- or RF-produced plasmas. Most such methods yield partially ionized plasmas whose electron density will change under laser irradiation. An exception may be the helicon-wave discharge in hydrogen (F. Chen, 1987); unfortunately, both this and the θ-pinch require magnetic fields, which are cumbersome and complicate the particle beam optics. To avoid collisional damping of plasma waves, $T_e > 100$ eV is desirable; inside the laser pulse, however, the large oscillating velocity of the electrons decreases their collisionality. The necessary degree of uniformity in n_o can be estimated as follows. By Eq. (23), the relativistic frequency shift is $\delta\omega = \varepsilon^2\omega_p/4$, and changes in ω_p over a stage length L should, therefore, be less than this. The density scalelength $L_n \equiv n_o/(dn_o/dx)$ must, therefore, be of order

$$L_n \simeq 2L/\varepsilon^2 \ , \qquad (41)$$

where a factor 2 accounts for $n_o \propto \omega_p^2$.

To keep the laser beams in focus, the stage length $L \cong L_a$ should be less than the Rayleigh length

$$L_R = 2\pi w_o^2 / \lambda_o \ . \qquad (42)$$

Let the minimum waist size w_o be *b* times c/ω_p. Eq. (6) than gives

$$L_R = b^2\gamma_p/k_p \ . \qquad (43)$$

Comparing this with $L_a = 2\gamma_p^2 / k_p$ [Eq. (33)], we see that $L_R/L_a = b^2/2\gamma_p$, which requires $b > (2\gamma_p)^{1/2}$.

To permit smaller radii, one can use relativistic self-focusing (Max et al., 1974) or hollow density profiles. The former comes about because electrons at the center of a Gaussian beam oscillate faster and are therefore heavier. This effect decreases ω_p and increases the index of refraction on axis, thus focusing the light, as verified in computer simulations by Forslund et al. (1985). The threshold

for relativistic self-focusing depends on power rather than intensity, and is given by Schmidt and Horton (1985) and by Sprangle et al. (1987) as

$$P_{sf} \cong 10\,(\omega_0/\omega_p)^2 \text{ GW}. \qquad (44)$$

For large γ_p, this threshold will not be reached, and one must keep the laser pulse focused by using an inverted density profile, which also acts as a positive lens. Because of the radial density gradient, the beat wave resonance is greatly modified. In the plasma fiber concept (Barnes et al., 1987), an electron density channel is created by the outward ponderomotive force of a single-frequency laser pulse (Felber, 1980), the ions being immobile. The channel traps the laser beam, acts as a slow-wave structure, an creates an axial component of $\underline{E}$ for acceleration.

Coulomb scattering of the particle beam by the plasma, leading to emittance growth, has been examined by Montague and Schnell (1985). At γ's of interest, they find that this effect is negligibly small.

Experiments

Excitation of plasma waves by optical mixing of laser beams was first demonstrated by Stansfield et al. (1971), and the density resonance was further verified for co-propagating beams by Joshi et al. (1982) and for counter-propagating beams by Amini and Chen (1984). Experiments on beat-wave acceleration are in progress in the United States (Joshi et al., 1987a,b), Canada (Martin et al., 1987), United Kingdom (Dangor et al., 1987), and Japan (Kitagawa et al., 1987). Using CO_2 laser light in the arrangement shown in Fig. 5, Clayton et al. (1985) excited a relativistic plasma wave ($\gamma_p = 10$) over a 2-mm length and measured its amplitude by ruby laser scattering. With $\alpha_0 = .017$ and $\alpha_2 = .034$, the results indicated $\epsilon \cong 3\%$, or $E_z \cong$ 1 GV/m, which is consistent with Eq. (12) when modified for finite risetime (Forslund et al., 1985).

4.8.3 Plasma Wake-field Accelerator

Basic concept

A relativistic particle traveling through a microwave cavity leaves behind an electromagnetic wake whose E_z field can be used to accelerate other particles (Ruth et al., 1985). The wake of a fast particle bunch in a plasma is an electrostatic plasma wave, which can be used for accelerating other particles to higher energies in the same manner as in the BWA. Using a particle beam for exciting an EPW avoids problems of laser inefficiency and density tuning. The concept, suggested by P. Chen et al. (1985, 1986), is illustrated in Fig. 6. In this figure, a nonuniform bunch of electrons (taken to be positive for clarity) is injected into a plasma at an energy $(\gamma_d - 1)mc^2$ of, say, 1 GeV. The wake consists of a plasma wave of frequency ω_p traveling with the bunch ($\gamma_p = \gamma_d$), so that $k \cong \omega_p/c$. The wave is loaded with a small bunch of particles injected at the proper phase for acceleration and focusing. The optimal density profiles are approximately triangular for both bunches. The wake of the driven bunch cancels the plasma wave, efficiently using its energy. Inside the driving bunch, electrons feel a small retarding field E^- from the wakes of the particles ahead; the bunch is shaped so that E^- is approximately constant. The driving bunch, therefore, loses all its kinetic energy in a distance $L = (\gamma - 1)mc^2 / eE^-$. If the maximum wake field is E^+, the driven bunch gains energy $\Delta\gamma mc^2 = eL|E^+|$. Thus, the driven particles have an energy gain larger than the driving energy by the ratio

$$R = |E^+ / E^-| \ , \qquad (45)$$

which is called the *transformer ratio*. For unshaped bunches, it can be shown that $R \le 2$; but for carefully shaped density profiles, R can be as large as 100. In this example, a low current, 100-GeV beam would be produced by a 1-GeV driving beam.

Plasma wakes in one dimension

Since the wake must travel with the driver, the problem is time-independent in the beam frame and can easily be solved in the one-dimensional case. Fig. 7 shows the wake of a charge sheet $\sigma\delta(z)$ moving to the left. In the beam frame,

the cold plasma streams by with a velocity $u\hat{z}$ and is set into oscillation with a velocity v and a perturbed density n_1. Setting $\partial/\partial t = 0$, we may write the equations of motion, continuity, and Poisson as

$$muv' = -eE \tag{46}$$

$$n_o v' + u n_1' = 0 \tag{47}$$

$$E' = -4\pi e n_1 = 4\pi\sigma\delta(z) , \tag{48}$$

where the prime indicates $\partial/\partial z$. Differentiating Eq. (48) and substituting Eqs. (46) and (47) yields

$$E'' + k_p^2 E = 4\pi\sigma\delta'(z) , \tag{49}$$

where $k_p^2 = \omega_p^2 / u^2 \cong \omega_p^2 / c^2$. The solution is easily verified to be

$$E = 4\pi\sigma \cos k_p z \, U(z) , \tag{50}$$

where U(z) is the step function $\int \delta(z)dz$. For shaped bunches $\rho(z)$, one integrates over this Green's function to obtain

$$E(z) = 4\pi \int_0^z \rho(z') \cos[k_p(z - z')] \, dz' . \tag{51}$$

A) *Case of constant* $\rho(z)$. Let the driving bunch be N wavelengths long, so that $\rho(z') = \rho_o$ for $0 \le z' \le d$, where $k_p d = 2\pi N$. Simple integration of Eq. (51) gives

$$E(z) = \frac{4\pi\rho_o}{k_p} [\sin k_p(d - z) + \sin k_p z] , \qquad z > d \tag{52}$$

$$E(z) = \frac{4\pi\rho_o}{k_p} \sin k_p z , \qquad z < d . \tag{53}$$

The maximum accelerating field in the wake occurs for $z = d/2 = 3\pi N/2k_p$, where Eq. (52) gives $E_m^+ = -2(4\pi\rho_o / k_p)$. The maximum retarding field inside the bunch is, from Eq. (53), $E_m^- = 4\pi\rho_o / k_p$. Thus unshaped bunches have R = 2. We note that the space charge of the beam itself has a maximum value $E_{sc} = \rho_o d/2$, which has been neglected though it is $k_p d / 8\pi$ times as large as E_m^-. This is a problem only in one dimension. In real beams of finite diameter, plasma electrons escape radially to cancel the space charge. In computer simulations which have verified the results of this section, plasma electrons have been removed artificially.

B) *Case of triangular* $\rho(z)$. Let $\rho(z') = \rho_o k_p z'$ for $0 \le z' \le d$, where $k_p d = 2\pi N$. The integral in Eq. (51) extends from 0 to z for $z \le d$ and from 0 to d for $z > d$ and is easily evaluated to give

$$E(z) = -\frac{4\pi\rho_o}{k_p} 2\pi N \sin k_p z , \qquad z > d \tag{54}$$

$$E(z) = \frac{4\pi\rho_o}{k_p} (1 - \cos k_p z) , \qquad z < d . \tag{55}$$

The transformer ratio in this case is obviously $R = 2\pi N/2 = \pi N$, which is >2 as long as $N > 1$.

The retarding field in Eq. (55) is not constant, as it should be for the highest efficiency, when all driving electrons lose all their energy simultaneously (Bane et al., 1985). Thus, we add a δ-function distribution $\sigma\delta(z)$, giving the E-field of Eq. (50), which cancels the $\cos k_p z$ term in Eq. (55) if $\sigma = \rho_o / k_p$. For the optimum distribution of a δ-function plus a triangle, which in practice can be approximated by the "doorstep" shape shown in Fig. 6, Eqs. (50), (54), and (55) give

$$E(z) = \frac{4\pi\rho_o}{k_p} (\cos k_p z - 2\pi N \sin k_p z) , \qquad z > d \tag{56}$$

$$E(z) = \frac{4\pi\rho_o}{k_p} = \text{const.} , \qquad z < d . \tag{57}$$

The maximum of Eq. (56) occurs for $\sin k_p z = -2\pi N \cos k_p z$, or $\sin k_p z = 2\pi N / [1 + (2\pi N)^2]^{1/2}$. Inserting these into Eq. (56) to obtain E_m^+ and dividing by $E_m^- = 4\pi\rho_o / k_p$, we obtain

$$R = [1 + (2\pi N)^2]^{1/2} \cong 2\pi N . \tag{58}$$

The fraction of the total charge that must be in the precursor for this optimal case is $\sigma / (\sigma + \frac{1}{2}\rho_o k_p d^2) = [1 + \frac{1}{2}(2\pi N)^2]^{-1} \cong 1/2\pi^2 N^2$. Since all driver particles except half of those in the precursor lose all their energy to the field E^-, it can easily be seen that the efficiency for conversion of beam energy to wave energy has the high value $[1 + (2\pi N)^2] / [2 + (2\pi N)^2]$.

Eq. (58) shows that a driver pulse which is slowly ramped in density over many plasma wavelengths can give a large transformer ratio. Fig. 8 shows a computer simulation verifying this result; other beam shapes have been investigated by Katsouleas (1986). Apparently, the physical effect of asymmetric pulses is the slow replacement of plasma electrons with beam electrons during the pulse. When the beam bunch suddenly ends, the large positive charge imbalance excites the plasma wave. In the one-dimensional problem, the cold electrons are given a beam-frame velocity $v = -(\rho_o / en_o)\omega_p z$ toward the head of the bunch, and the precursor serves to impart an acceleration that sets up this motion. In two dimensions, the cold electrons can easily be driven out sideways to preserve charge neutrality.

Two-dimensional wakes and instabilities

The wake of a point charge q with charge density $q\delta(r)\delta(z) / 2\pi r$ can be found in a similar fashion (Katsouleas et al., 1987a). We now transform to the laboratory frame (r, θ, z_l) by replacing z by $z_l + ut$ in Fig. 7. The result is

$$E_z = 2qk_p^2 K_o(k_p r) \cos[k_p(z_l + ut)]U(z_l + ut) , \qquad (59)$$

where K_o is a modified Bessel function. In addition, there is now a radial component E_r, which can be found from the θ component of Faraday's Law:

$$-\frac{1}{c}\frac{\partial B_\theta}{\partial t} = \frac{\partial E_r}{\partial z_l} - \frac{\partial E_z}{\partial r} . \qquad (60)$$

Though $u \equiv c$ in practice, we have for clarity neglected retardation and the Lorentz transformation of $\underline{E}_\perp$ and $\underline{B}_\perp$. Since the pattern of Fig. 7 moves with velocity $-u\hat{z}$ in the lab frame, we have $\partial B_\theta / \partial t = u\partial B_\theta/\partial z_l$, so that Eq. (60) becomes

$$\frac{\partial}{\partial z_l}(E_r + \frac{u}{c} B_\theta) = \frac{\partial E_z}{\partial r} . \qquad (61)$$

It is customary to define the wake function $\underline{W} = \underline{E} + \frac{1}{c}\underline{v}_b \times \underline{B}$, where the beam velocity v_b is $-u$ in this case. Thus $W_{||} = E_z$ and $W_\perp = E_r + (u/c)B_\theta$ in axisymmetric cases. Eq. (59) can be differentiated in r, using $K_o'(x) = -K_1(x)$, and integrated over z_l to obtain

$$W_\perp \equiv E_r + B_\theta = -2qk_p^2 K_1(k_p r) \sin[k_p(z_l + ut)]U(z_l + ut) . \qquad (62)$$

In vacuum cavities, B_θ is comparable to E_r; but in a plasma, $|B_\theta|$ is small compared with $|E_r|$ because the wave is electrostatic. The focusing force on a particle traveling with $\underline{v}_b$ is proportional to $W_\perp$. In Fig. 6, the driven bunch is placed in a phase where $qE_r < 0$ for focusing. Particles which move relative to the wave will feel an alternating force and are subject to strong focusing, an effect applicable to final focus techniques (P. Chen, 1986).

From Eqs. (59) and (62) it is seen that the radial extent of the wake is $k_p^{-1} \equiv c/\omega_p$ even for a point charge. Using Eqs. (59) and (62) as Green's functions, one can calculate the parallel and transverse wakes of any axisymmetric charge distribution of radius a (Katsouleas et al., 1987a; Ruth et al., 1985; P. Chen et al., 1987). As expected, the wake radius is of order a if $a \gg c/\omega_p$ and of order c/ω_p if $a \leq c/\omega_p$. A simple cartesian treatment can be found in Wilks et al. (1987).

Because of their self-generated magnetic fields, finite-radius beams are subject to whole-beam self-focusing (or pinching) if $a \leq c/\omega_p$ and to filamentation (also called tearing or Weibel instability) if $a \gg c/\omega_p$. The two-stream instability between the beam electrons and the plasma electrons also can limit the transformer ratio even in the one-dimensional case. These instabilities have been analyzed by Keinigs and Jones (1987) and by Su et al. (1987). Simulations by the latter authors show that these instabilities can be suppressed by giving the driving bunch a transverse energy spread of about 25 KeV.

Beam loading and shaping

We now show that the energy of the plasma wave can be converted efficiently into particle energy. The wake of an ideal driver is a sine wave [Eq. (54)], as is the wake of an infinitely short bunch of driven particles [Eq. (50)]. It is then clear that a short driven bunch of appropriate density can be injected at a proper phase so that its wake exactly cancels the wake of the driver, and thus it can be accelerated with 100% efficiency. Unfortunately, the energy spread would also be 100%, since particles at the tail of the bunch would feel no accelerating field. To minimize energy spread, one must shape the bunch density so that the

field inside the driven bunch is constant. As with the driver, this can be done with a triangular profile, but reversed, as shown in Fig. 6.

Referring to Fig. 7, let the wake field be given by $E(\zeta) = E_o \cos\zeta$, where $\zeta = k_p z = k_p(z_l + ut)$., Let the driven bunch have a charge density $\rho_b(\zeta)$ of the form

$$\rho_b(\zeta) = \rho_o + \rho_1(\zeta_o - \zeta), \qquad \zeta_o < \zeta < \zeta_1 \tag{63}$$

The self-field inside the bunch is given by Eq. (51):

$$E_{self} = \frac{4\pi}{k_p} \int_{\zeta_o}^{\zeta} \rho_b(\zeta') \cos(\zeta - \zeta')d\zeta'. \tag{64}$$

Inserting Eq. (63) and integrating gives

$$(k_p/4\pi)E_{self} = \rho_o \sin(\zeta - \zeta_o) - \rho_1[1 - \cos(\zeta - \zeta_o)]. \tag{65}$$

Adding the wake field $E_o \cos\zeta$, one obtains the total inside field

$$(k_p/4\pi)E_{in} = -\rho_1 + [(k_p/4\pi)E_o - \rho_o \sin\zeta_o + \rho_1 \cos\zeta_o]\cos\zeta$$

$$+ [\rho_o \cos\zeta_o + \rho_1 \sin\zeta_o]\sin\zeta \ . \tag{66}$$

To obtain constant E_{in}, ρ_o and ρ_1 must be such that the coefficients in brackets vanish. These conditions give

$$\rho_o = (k_p/4\pi)E_o \sin\zeta_o, \qquad \rho_1 = -(k_p/4\pi)E_o \cos\zeta_o \ , \tag{67}$$

so that the height and the slope of $\rho_b(\zeta)$, but not its length, are prescribed.

We now have

$$\rho_b(\zeta) = (k_p/4\pi)E_o[\sin\zeta_o + (\zeta - \zeta_o)\cos\zeta_o], \tag{68}$$

$$E_{in} = E_o \cos\zeta_o \ . \tag{69}$$

Again assuming positive electrons, we see that E_{in} is accelerating if $\cos\zeta_o < 0$ [see Fig.7] and that ρ_b changes sign at $\zeta = \zeta_m$ given by

$$\zeta_m - \zeta_o = -\tan\zeta_o \ . \tag{70}$$

Thus the bunch must be injected with $\pi < \zeta_o < 3\pi/2$, and its length $\zeta_1 - \zeta_o$ must be less than $\zeta_m - \zeta_o$. It is clear that setting $\zeta_1 = \zeta_m$ gives the largest number N of particles/cm^2 in the bunch. Then N is given by

$$N = \frac{1}{ek_p} \int_{\zeta_o}^{\zeta_m} \rho_b(\zeta)d\zeta = -\frac{\sin^2\zeta_o}{2\cos\zeta_o} \frac{n_1}{k_p} \ , \tag{71}$$

where $n_1 = k_p E_o/4\pi e$ is the plasma wave density fluctuation. The choice of ζ_o is compromise between accelerating gradient [Eq. (69)] and either N or efficiency η. The latter is found by calculating the field behind the bunch, using Eq. (64) with limits ζ_o and ζ_m, and adding $E_o \cos\zeta$, with the result

$$E_{out} = E_o \cos\zeta_o \cos(\zeta_m - \zeta) = E_{in} \cos(\zeta_m - \zeta) \ . \tag{72}$$

Thus the energy left in the wave is $E_{in}^2/8\pi$, and the efficiency is

$$\eta_{load} = (E_o^2 - E_{in}^2)/E_o^2 = \sin^2\zeta_o \ . \tag{73}$$

For example, with $\zeta_o = 240°$ and density $n_1 = n_o = 10^{17}$cm^{-3}, one can approach 75% efficiency with $|E_{in}| = 0.5\ E_o$ and 1.3×10^{14} particles per bunch, with zero energy spread. A computer simulation of this case is shown in Fig. 9, together with evidence of small energy spread.

This energy spread, as well as the emittance, of any finite-diameter beam will be subject to the two-dimensional effects of Eqs. (59) and (62). Radial inhomogeneities can be minimized by making the driven beam much narrower than the wake field, which can have a radius no smaller than c/ω_p. Since the wake of even a point charge is $\simeq c/\omega_p$ wide [Eq. (59)], a bunch with radius $a \ll c/\omega_p$ can

effectively cancel the wake field over its entire cross section, achieving a loading efficiency not much smaller than that of a wide bunch; details are given by Katsouleas et al. (1987a). As a practical example, the latter consider a plasma wave of amplitude $\epsilon = 0.5$ in a density $n_o = 10^{16}\text{cm}^{-3}$ (giving $c/\omega_p \cong 50\,\mu\text{m}$ and $E_o \cong 5$ GV/m), loaded with a bunch of radius $a = 0.2\,\mu\text{m} = .004/k_p$ containing 6×10^8 electrons, with an injection phase $\sin\zeta_o = 0.2$. The small value of $\underline{a}$ permits the emittance (defined in Sec. 4.8.7) to be 10^{-12} cm-rad, allowing a final focus of 100 Å radius and a luminosity (Sec. 4.8.7) of $\cong 10^{33}\,\text{cm}^{-2}\,\text{sec}^{-1}$ at a 5 kHz repetition rate and a disruption parameter of 2.

The optimal pulse shapes derived above can be approximated by using photocathode electron sources illuminated by time-shaped laser pulses (Fraser, 1987). In addition, a self-sharpening effect occurs because particles coming after the abrupt end of the drive pulse [cf. Fig.6] are accelerated by the E_z field and are brought into the main bunch. Katsouleas et al. (1987b) have shown by simulation that a Gaussian bunch of width σ can be sharpened by a density giving $k_p = \omega_p/c = 7/\sigma$. A further beneficial effect occurs if the plasma wave is driven to an amplitude so large that the nonlinear frequency shift [Eq. (23)] appreciably reduces k_p at the end of the pulse. Transformer ratios > 2 can then be obtained even with unshaped bunches (Rosenzweig, 1987) because the change in k_p causes even a symmetric bunch to appear to be sharper near its tail relative to the local wavelength (Katsouleas et al., 1987b). Focused bunch densities may exceed n_o. The value of ω_p, and thus of k_p, can also be changed by a gradient in the background density n_o. Since wake fields are generated at any density, the PWFA has an advantage over the BWA in that the phase slippage of the accelerating particles can be compensated by tailoring the density profile.

Experiment

No experimental results on the PWFA yet exist, but a test is planned at the Argonne National Laboratory in Illinois, U.S.A. in a collective effort with the University of Wisconsin (Rosenzweig et al., 1985, 1987; Keinigs et al., 1987). In this experiment, a linac produces both a 6-psec, 22-MeV driving bunch at 1.2 msec intervals and a 15-MeV witness beam which can be delayed by varying the time of flight so that it can be injected at various phases into the wake. The plasma of 10^{12}–10^{14} cm^{-3} density is produced by a 20-cm long hollow cathode arc in an 800 G field. Radial effects can be studied by offsetting the witness beam, and beam shaping can also be investigated.

4.8.4 Plasma Wave Nonlinearities

Nonlinear frequency shift

Both the BWA and the PWFA are sensitive to the nonlinear behavior of plasma waves. Perhaps the most fundamental point is the frequency shift at large amplitudes, a critical factor in the derivation of the Rosenbluth-Liu formula, Eq. (12). For nonrelativistic motions, Dawson (1959) showed that the frequency ω_p is unchanged up to wave breaking; and for the relativistic case, Akhiezer and Polovin (1955) showed that the only change is a redshift due to the mass increase [Eq. (21)]. That all other nonlinearities cancel is, however, a subtle point which has only recently been clarified by McKinstrie and Forslund (1987) and by Mori (1987a). The source of discrepancies in the literature (referenced by the foregoing authors) lies in the dc component of the second order current $j^{(2)} = n_1 v_1 + n_o v^{(2)}$. Ampère's Law $c\,\underline{\nabla}\times\underline{B} = 4\pi\underline{j} + \partial\underline{E}/\partial t = 0$ shows that $j_{dc} = 0$ for electrostatic waves, so that the sum of $\langle n_1 v_1\rangle$ and $n_o v_{dc}^{(2)}$ must vanish. If $v_{dc}^{(2)}$ is arbitrarily set equal to 0, a spurious blue shift is obtained due to the Doppler effect of $\langle n_1 v_1\rangle$. There is, of course, a blue shift due to thermal motions in both the linear (Bohm-Gross) and nonlinear regimes.

Wavebreaking amplitude

As plasma waves become large, their wavefronts steepen until the electron fluid velocity v becomes comparable to the phase velocity v_p, and the particle positions become double-valued. This "wavebreaking" limit for cold, nonrelativistic plasmas is given by Dawson (1959) as

$$eE_{max}/m\omega_p v_p = 1 \quad , \tag{74}$$

which coincidentally agrees with the naive equation (7) even though E_{max} and ϕ_{max} are no longer trivially related because of the development of harmonics. When finite T_e is introduced, E_{max} is reduced because the electron pressure resists compressions, and because thermally moving electrons are more easily trapped. Coffey(1971) gives the warm-plasma, non-relativistic limit

$$eE_{max}/m\omega_p v_p = (1 - 8\alpha_t^{1/4}/3 + 2\alpha_t^{1/2} - \alpha_t/3)^{1/2} \quad , \tag{75}$$

where $\alpha_t \equiv 3KT_e/mv_p^2$. Relativistic plasma waves with $v_p \cong c$ can have amplitudes much larger than this because the electrons become heavy ($v \cong c$) near wavebreaking and their orbits cannot easily overlap. Akhiezer and Polovin (1956) give for the $T_e = 0$ case

$$eE_{max}/m\omega_p c = 2^{1/2}(\gamma_p - 1)^{1/2} \tag{76}$$

for $\gamma_p = 100$, this predicts a value 14 times larger than the non-relativistic amplitude. However, Katsouleas and Mori (1987) have found that thermal effects lessen the effect. For $\alpha_t \ll 1$ and $\gamma_p \gg 1$, they obtain

$$eE_{max}/m\omega_p c \simeq \alpha_t^{-1/4}[\ln(2\gamma_p^{1/2}\alpha_t^{1/4})]^{1/2} \quad , \tag{77}$$

which is 8.55 at $KT_e = 10$ eV, $\gamma_p = 100$. Though this value is larger than unity, even the latter may be unattainable because of instability limits.

Steepening and harmonics

Since the equation of continuity for longitudinal waves [Eq. (16)] gives $\underline{v}_1 = (n_1/n_o)\underline{v}_p$, there is a nonlinear effect causing electrons to move forward in the wave frame wherever $n_1 > 0$ and backward wherever $n_1 < 0$. This has the effect of bunching the density into striations and steepening the E-field sine wave into a sawtooth shape, thus generating harmonics in the ω and k spectra (Dawson, 1959). The relative amplitudes of these harmonics in the nonrelativistic case have been given by Jackson (1960) and by Koch and Albritton (1975) for $T_e = 0$ and may be summarized as follows (Umstadter et al, 1987):

$$\frac{n_m}{n_o} = c_m\left(\frac{n_1}{n_o}\right)^m \quad , \qquad c_m \equiv \frac{m^m}{2^{m-1}m!} \quad . \tag{78}$$

Thus $c_1 = 1$ is the linear amplitude by definition, $c_2 = 1.0$ is the coefficient for the second harmonic at $2\omega_p$, $2k_p$, and so forth. When kinetic effects are taken into account for $T_e > 0$, Kuz'menkov et al. (1983) give modified values of c_m; for instance, for $KT_e = 10$ eV, $v_p/c = 0.02$, one finds $c_2 = 1.3$, $c_3 = 1.9$. In addition, there are particle trapping effects, which have been studied extensively in the computer simulations of Buchel'nikova and Matochkin (1987). Steepening of relativistic waves has been shown by Rosenzweig (1987). The change in wave shape does not in itself remove energy from the wave but does affect the phase in which accelerated particles must be injected.

An experiment to detect steepening in a laser-driven wave has been reported by Umstadter et al. (1987). Stimulated Raman scattering of 10.6–μm laser light was used to generate intense plasma waves in an apparatus similar to that of Fig. 5. Thomson scattering of a ruby laser beam (0.69 μm) was detected at scattering angles of 7°, 14° , and 21°, corresponding to the harmonics c_1, c_2, c_3 defined above. Fig. 10 shows the relative amplitudes n_2/n_o and n_3/n_o, in agreement with the dependence predicted by Eq. (78) and the coefficients computed from Kuz'menkov et al. (1983).

Mode coupling

Plasma accelerators, particularly the beat-wave accelerator, are sensitive to deviations from uniform density. In the BWA, an inhomogeneity in the form of a density ripple often arises because stimulated Brillouin scattering of either pump beam has a low threshold and excites an ion acoustic wave of typical amplitude $n_1/n_o = 1$ to 10%. For simplicity, we may assume the ion wave frequency to be essentially zero so that, from Eq. (1), the ripple is stationary with wave number $k_i = 2k_o$. The plasma wave is then described by the equation

$$\left[\frac{\partial^2}{\partial t^2} + \omega_p^2(z) - 3v_e^2\frac{\partial^2}{\partial z^2}\right]n_1 = C\,E_o E_2 \quad , \tag{79}$$

where $v_e^2 = 3KT_e/m$, C is a coupling coefficient, E_o and E_2 are light waves, and $\omega_p^2(z)$ has the form $\omega_p^2(z) = \omega_{po}^2(1+\epsilon_i \cos 2k_o z)$. This equation was solved by Kaw et al. (1973) for the undriven case C = 0, by Darrow et al. (1986,1987) for the beat-wave case with E_o and E_2 given, and by Barr and Chen (1987) for the stimulated Raman instability, where E_o is a pump but E_2 is driven and follows a similar coupled equation.

In all cases the effect of the ripple is to couple energy from the fundamental mode (ω_p, k_p) into other modes with $\omega = \omega_p$, $k_m = k_p \pm mk_i$. In the BWA where $\underline{k}_o$ and $\underline{k}_2$ are in the same direction, Eq. (3) gives $k_p \cong \omega_p/c \ll 2k_o$; hence, the coupled modes are slow waves in either direction with $|v_p| \cong \omega_p/k_i$. In Raman backscatter (which occurs as an undesired process in the BWA), $\underline{k}_o$ and $\underline{k}_2$ are in opposite directions, and $k_p \cong -2k_o - \omega_p/c \leq k_i$. This special case, with $k_p \cong k_i$, has interesting consequences pointed out by Barr and Chen (1987). One of these, the existence of a backward slow wave ($k \cong -k_i$) of large amplitude, has been confirmed experimentally (Umstadter, 1987).

In the case of relativistic plasma waves with $k_p \cong \omega_p/c = k_o/\gamma_p$, Darrow et al. (1987) show that the coupled modes oscillate in time and can be expressed as sums of Bessel functions $J_m(\epsilon_i \omega_{po} t/2)$. Fig. 11 shows the behavior of the first four modes. Loss of energy to these modes can cause the beat wave to saturate at a level below that predicted by relativistic detuning [Eq. (12)]. Darrow et al. (1987) find that mode coupling dominates at low intensities such that $\alpha_o \alpha_2 < [1.6\epsilon_i/f(T_e)]^{3/2}$, where $f(T_e)$ is of order unity.

Coupled modes have been detected in a beat-wave experiment in the presence of Brillouin scattering (Darrow et al., 1986, 1987). Fig. 12 shows waves of various ω and k detected by ruby laser Thomson scattering. In this experiment, both SRS and SBS occurred separately for each of the CO_2 laser pump beams, creating reflected beams strong enough to become secondary pumps. Thus, in addition to mode coupling, various processes of optical mixing between co- and counter-propagating pumps are also possible, and analysis is difficult. However, by using picosecond pulses, SBS, ripple formation and other instabilities involving the slow motion of ions can be suppressed.

Modulational and decay instabilities

A modulational instability is the tendency for a ripple in the envelope of wave intensity to grow, causing even a plane wave to have large fluctuations in amplitude. It is well known (Mima and Nishikawa, 1984) that instability requires the nonlinear frequency shift $\Delta\omega/\Delta|E^2|$ to have opposite sign to the group dispersion $\Delta v_g/\Delta|k|$. Since the latter is > 0 for a plasma wave ($v_g \cong 3kv_e^2/\omega_p$), the relativistic redshift of EPW's causes them to be modulationally unstable. This effect, however, is weak compared with the redshift which occurs on time scales long enough for ions to move. In that case, the ponderomotive force pushes plasma away from regions of large $|E^2|$ and thus lowers the local value of ω_p. The importance of this instability to plasma accelerators has been pointed by Bogomolov et al. (1987) and examined in detail by Pesme et al. (1987), who found growth rates as large as ω_{pi}^{-1}. Since ω_{pi}^{-1} = 2.4 psec for hydrogen at $n_o = 10^{17}\,cm^{-3}$, very short pulses are required to avoid such effects. Related to the modulational instability, which is a non-resonant, four-wave process, is the resonant, three-wave process of parametric decay into an ion wave and a lower-frequency plasma wave. The small value of k_p in relativistic plasma waves, however, causes the coupling to ion waves to be rather weak. Experimental evidence of these phenomena is embodied in the extensive literature on envelope solitons, cavitons, and collapse. The strong effect of the ponderomotive force of a two-dimensional EPW manifests itself in the resonant self-focusing phenomenon noticed in the beat-wave experiment of Joshi et al. (1982).

4.8.5 Instabilities

The most important plasma instabilities have already been discussed in the relevant sections; here, we give a catalog of known instabilities found in the work of Mori (1987) and Bingham et al. (1987). Table 1 lists instabilities by the energy source that drives them. Those in the first column involve only electron motions and may have fast growth rates; those in the second column involve ion motions and can be avoided by using sufficiently short pulses. The wake-field accelerator avoids all the laser-driven instabilities.

The stimulated Raman and Brillouin backscatter instabilities have well-known thresholds and growth rates, which are *modified* when the laser intensity is high enough to affect the electrostatic wave dispersion relation, and when Landau damping causes the decay wave to be in the *Compton* (single-particle) regime. Raman forward scatter is a four-wave process similar to self-focusing. The latter is the same as filamentation except that it involves the whole laser beam. Self-modulation is a change of intensity in the axial rather than the radial direction. The relativistic and ponderomotive mechanisms both change the value of ω_p; the former by increasing m and the latter by decreasing n_o.

In accelerators, the parametric decay and ion-acoustic instabilities involve long-wavelength ion waves, which grow slowly. The sausage and firehose pinch instabilities cannot take place with short bunches. The other beam instabilities can be suppressed by transverse temperature. The most troublesome instability for the BWA is likely to be SRS; and for the PWFA, the ponderomotive modulational instability. No instability has been shown to be an insuperable obstacle.

4.8.6 Cross-field accelerators

The phase slip of an accelerating particle in a plasma wave can be eliminated by the addition of a uniform, dc magnetic field $\underline{B}_o$. Arbitrarily long stage lengths are then possible, limited only by pump depletion. Suggested by studies of wave damping (Sagdeev and Shapiro, 1973; Dawson et al., 1983), this idea has been worked out by Katsouleas and Dawson (1983), Sugihara et al. (1984), and Gribov et al. (1985). It has been named the "surfatron" by Katsouleas and Dawson (1983) and "$v_p \times B$ acceleration" by Sugihara et al. (1984). Consider the geometry of Fig. 13a, in which a particle being accelerated in a plasma wave with $\underline{v}_p$ in the x direction is subject to a field $\underline{B}_o$ in the z direction. The Lorentz force $F_y = -qv_xB_o/c$ gives the particle a velocity in the -y direction; and v_y, in turn, exerts a Lorentz force in the -x direction which prevents the particle from slipping forward in phase relative to the wave. Though the Lorentz force cannot give energy to the particle, it helps by keeping the particle at the position of maximum E_x. The particle is thus constrained to have $v_x = v_p$, but its γ can increase because its total velocity is at an angle $\theta = \tan^{-1}v_y/v_x$ (the "surfing angle") relative to the wave. This angle is shown in Fig. 13b, which also shows how a particle injected at an arbitrary phase will oscillate about its equilibrium position in the wave. These oscillations are damped as the particle approaches the light cone, partly because of conservation of action and partly because of its increase in mass. Therefore, in addition to unlimited acceleration, the surfatron offers the second advantage of a narrow energy spread.

In the wave frame moving with v_p, the field B_o transforms to $B_o' = \gamma_p B_o$, while the longitudinal field E_o is unchanged. The Lorentz force $F_x' = qv_yB_o'/c$ can never exceed the electrostatic force qE_o if $E_o > \gamma_pB_o$, since $v_y < c$. Thus, particles always remain trapped if $E_o > \gamma_pB_o$ or, from Eqs. (7) and (8), if $\omega_c < \epsilon\omega_p/\gamma_p$. From the triangle in Fig. 13b, we see that $v_y = c(1-\beta_p)^{1/2} = c/\gamma_p$ after the particle reaches large γ, and therefore the angle θ is given by $\sin\theta \cong \theta \cong v_y/c = 1/\gamma_p$. From the relativistic theory given by Katsouleas and Dawson (1983) and Katsouleas (1984), the energy gain is $\Delta\gamma/\Delta x \cong \epsilon k_p$. For example, to obtain 1 GeV electrons, one could beat CO_2 laser beams in a plasma of $10^{17}\,cm^{-3}$ density in a 20-kG magnetic field. One then has $\gamma_p = 10$ and $\theta = 5.7°$; and if $\epsilon = 0.2$, $\Delta\gamma = 2000$ is reached in a distance $\Delta x = 17$ cm.

Since the particles move laterally a distance $\Delta y = 1.7$ cm in the above example, the plasma wave must have that width unless it can be made to follow the particle beam rather than the phase velocity $\underline{v}_p$. This can indeed be done by *finite-angle optical mixing* of laser beams at an angle $\phi \cong \gamma_p^{-3}$ (F. Chen, 1985). Only one of the laser beams then needs to be defocused to cover the acceleration region. Another finite-angle effect has been pointed out by Sugihara et al. (1984) and extended to the relativistic case by Sakai et al. (1984). If the field $\underline{B}_o$ is at an angle $\psi \neq \pi/2$ relative to $\underline{k}_p$, the acceleration gradient is larger for given E_o/B_o than for $\psi = \pi/2$; but the ultimate value of γ is no longer infinite.

Experimentation on the $v_p \times B$ effect has been done only in the microwave regime. Using 2.86-GHz microwaves to excite plasma waves by resonance absorption in a large filament-discharge plasma with $n_o = 2\times10^{11}\,cm^{-3}$, Nishida et al. (1985, 1987) observed an increase in the hot-electron current when a transverse magnetic field $B_o \leq 11$ G was applied. The hot electron flux

($\cong$ 90 eV) is directed in the $-ev_p \times B_o$ direction and shows a peak for values of B_o near the non-relativistic trapping limit $E_o/B_o \cong v_y/c$. In a subsequent experiment, Nishida and Sato (1987) also demonstrated the beneficial effect of varying the angle ψ.

4.8.7 Plasma lenses

The final focus in linear colliders presents challenging problems to the plasma physicist. In an unneutralized, cylindrical beam, the outward space charge force qE_r at radius r is $qE_r = 2\pi rq^2\bar{n}$, where $\bar{n}$ is the average density inside radius r. The inward Lorentz force is $-(q/c)v_z B_\theta = -2\pi rq^2\bar{n}(v_z^2/c^2)$, since $B_\theta = 2I/rc$ and $I = \pi r^2 \bar{n} q v_z$. Thus, for relativistic beams ($v_z \cong c$) these forces cancel at all radii. At the focus of an $e^+ - e^-$ collider, however, there is no space change if the beams are of equal density, and the pinch forces are uncompensated. The effect of the pinch force in focusing the beams is characterized by the *disruption parameter* D:

$$D \equiv \left[\frac{e^2}{\gamma mc^2} \frac{NL}{r_o^2} \right] , \qquad (80)$$

where N is the number of particles in a bunch of length L and radius $\cong r_o$. This can be understood by considering the pinch force $F_r = -4\pi re^2\bar{n}$ on a particle due to the B_θ of both bunches. In traveling for a time $t = L/c$ through the focus, a particle of mass γm is displaced radially by the distance $\Delta r = (Fr/2\gamma m)t^2 = -(e^2/\gamma mc^2)(2\pi rL^2\bar{n})$. Since $N = \pi r^2 L\bar{n}$, the fractional displacement is $-\Delta r/r = (e^2/\gamma mc^2)(2NL/r^2)$, which is essentially D. For $D > 1$, the focal radius is radically modified.

The *luminosity* is defined as $\mathscr{L} = R/\sigma$, where R is the number of collisions of cross section σ per second. If f is the repetition rate of colliding bunches containing N particles, then R is clearly $N^2 f(\sigma/A)$, where A is the effective cross-sectional area of each bunch. For Gaussian bunches of density $n_o \exp(-2r^2/r_o^2)$, one obtains

$$\mathscr{L} = N^2 f H / 4\pi r_o^2 . \qquad (81)$$

Here we have included the pinch-enhancement factor H, which must be computed numerically as a function of D for real beam profiles. In practice, $\mathscr{L}$ is limited by the speed of detectors to a useful value not much in excess of $10^{33}\,cm^{-2}\,sec^{-1}$, and H is no larger than about 5 regardless of D. If $N = 3\times10^9$ and $F = 2$ kHz, we see that this luminosity requires $r_o \cong 250$ Å. Two effects limit the fineness of focus: the beam's "emittance" (analogous to diffraction in optical systems) and the aberration of the lens. Plasma techniques may help to achieve the required spot sizes and to center the beams.

Emittance is a measure of angular spread. If a focusing force is applied to a particle which is off-axis, it will undergo "betatron" oscillations, defined as follows. Let the particle travel with velocity $\cong c$ in the z direction and be pushed toward the axis by a force F_y, whose linear term near the axis can be written $F_y = -\beta_1 y$. The equation of motion $\gamma m\ddot{y} = -\beta_1 y$ has the obvious solution $y = y_o \exp[\pm i(\beta_1/\gamma m)^{1/2} t]$. Since $z \cong ct$, we may write $y = y_o \exp(\pm ik_\beta z)$, where the betatron wavelength λ_β is given by

$$\lambda_\beta = 2\pi/k_\beta , \quad k_\beta^2 = \beta_1/\gamma mc^2 . \qquad (82)$$

The particle moves in an ellipse in v_y–y phase space, exchanging potential and kinetic energy. It is customary to use y′–y phase space, where $y' = \partial y/\partial z = v_y/c = \pm ik_\beta y$ is essentially the angle of the orbit to the axis. A distribution of particles will occupy an area

$$\varepsilon_y = (\Delta y)(\Delta y') = k_\beta (\Delta y)^2 \qquad (83)$$

in y′–y space, call the *emittance*, which is invariant if the motion conserves energy. Changing k_β changes the shape of the ellipse but not its area. A similar emittance ε_x is defined for the x motion, and we consider $\varepsilon_x \cong \varepsilon_y$.

Damping rings remove energy by synchrotron emission, thus lowering ε_y and the possible focal width Δy. In principle, plasma particles could also remove energy, but a more efficient mechanism is available. The plasma lens does not change ε_y but instead increases F_y and k_β to lower Δy. Fig. 14 shows the operation of a non-optimized lens. The force F_y is just the transverse wake function $W_\perp$ in Eq. (62). It is clear that F_y is not the same for all parts of the beam in Fig.

14, but the beam shape can be optimized in the same way as in the beam loading problem. For constant *transverse* force, it turns out that the required shape is a constant density bunch following $\lambda_p/4$ behind a δ–function precursor. For such a bunch of radius a and length b, containing N electrons, P. Chen et al. (1987) find that

$$k_\beta^2 = \frac{W_\perp'/r}{\gamma mc^2} = \frac{e^2}{\gamma mc^2}\,\frac{4Nk_p}{a^2\,(1+k_pb)} \quad . \tag{84}$$

This force can be applied in a thin lens or a thick lens. In a thin lens, the beam is given a focusing force in a length l of plasma separated a focal distance $L_f \gg l$ from the high-vacuum interaction region. The strength of $W_\perp$ greatly shortens L_f and hence decreases the spot size. For instance, a 5–TeV e^+ or e^- beam of emittance $\gamma\varepsilon_y = 4\times10^{-8}$ m–rad with $a = 3$ μm and $b = 100$ μm passing through a 23-cm long lens with $n_o = 10^{18}$ cm^{-3} will be focused to a radius of 20 Å in a distance $L_f = 4.8$ m (P.Chen et al., 1987). The focusing force is equivalent to a magnetic field gradient of 830 MG/cm. A thick lens is one which envelopes the focal point, so that high-energy events occur in the presence of plasma. The motion is so nonlinear that one must depend on computer simulations, such as the one shown in Fig. 15.

If F_y contained only the linear term $-\beta_1 y$, the plasma lens would have no aberration, but in practice the nonlinear terms, which *increase* with the radius a of the bunch entering the lens, cause an aberration which limits the spot size. The emittance is a relatively small effect for large–γ beams. As in diffraction, the emittance-limited spot size is proportional to the f-number $f = L_f/a$ and therefore *decreases* with a. Since aberration is dominant, plasma lenses are best used with small a, serving as a final focus device after focusing by conventional quadrupoles.

4.8.8 Related concepts

In the original work of Tajima and Dawson (1979), a single laser pulse rather than a coherent EPW was envisioned. *Triple solitons* (Nishihara, 1975) are pulses which can contain two beating laser beams and a plasma wave, phased in such a way as to leave no wake (Mima et al., 1986; McKinstrie and DuBois, 1986; McKinstrie, 1988). The energy of the EPW is given back to the light waves at the end of the pulse, thus increasing the pump depletion distance. However, loading was not considered.

Another solution to the pump depletion problem is to use *converging plasma waves* (Katsouleas et al., 1985a), in which two beat waves are directed at an angle to the axis (Fig. 16). The interference pattern on the axis has a phase velocity faster than v_p which can be adjusted between stages to account for phase slip. The *plasma waveguide* or *plasma fiber* accelerator (Barnes et al., 1987) is essentially the same idea, except that the EPW is a finite-geometry eigenmode with large $\omega/k_{\parallel}$.

The *plasma grating accelerator* (Katsouleas et al., 1985b) provides another way to generate EPW's of arbitrary phase velocity. Consider an ion acoustic wave (ω_i , k_i) propagating in the z direction and a laser beam (ω_o , k_o) propagating in the y direction with $\underline{E}$ in the z direction. The oscillating electrons in the laser beam will cause space charges to build up in the density ripple. The resulting electrostatic field has frequency $\omega \cong \omega_o$ and $k \cong k_i$ and can be decomposed into two counterpropagating plasma waves. This is essentially an oscillating two-stream instability seeded with an ion ripple.

Acknowledgments

This work was supported by the National Science Foundation, Grant No. ECS83-10972 and by the Department of Energy, Contract No. DE-AS03-83-ER40120.

References

Akhiezer, A.I., and R.V. Polovin, 1955, Dokl. Akad. Nauk SSSR 102, 919.

Akhiezer, A.I., and R.V. Polovin, 1956, Sov. Phys. JETP 3, 696.

Amini, B., and F.F. Chen, 1984, Phys. Rev. Letters 53, 1441.

Baldis, H. A., 1988, this volume.

Bane, K.L.F., P. Chen , and P. B. Wilson, 1985, IEEE Trans. Nucl. Sci., NS-32, 3524.

Barnes, D.C., T. Kurki-Suonio, and T. Tajima, 1987, in: Katsouleas, 1987 (loc. cit.), p. 154.

Barr, H.C., and F.F. Chen, 1987, Phys. Fluids 30, 1180.

Bingham, R., W.B. Mori, and J.M. Dawson, 1985, in: Joshi and Katsouleas, 1985 (loc. cit.), p. 138.

Bogomolov, Ya.L, A.G. Litvak, and A.M. Feigin, 1987, Proc. Int'l Cong. on Plasma Physics, Kiev, USSR, Vol. 1, p. 76.

Bryant, P., and J.H. Mulvey, eds., 1984, Workshop on Generation of High Fields for Particle Acceleration to Very High Energies, Frascati, 1984 (Report 85/91, European Committee for Future Accelerators).

Buchel'nikova, N.S., and E.P. Matochkin, 1987, Proc. Int'l Conf. on Plasma Physics, Kiev, USSR, 1987, Vol. 2, p. 128.

Channel, P.J., ed., 1982, Workshop on Laser Acceleration of Particles, Los Alamos, 1982 (Conference Proceedings No. 91, American Institute of Physics, New York).

Chen, F. F., 1974, in: Laser Interaction and Related Plasma Phenomena, H. J. Schwarz and H. Hora, eds. (Plenum, New York), Vol. 3A, p. 291.

Chen, F.F., 1985, Proc. XII Int'l Symposium on Physics of Ionized Gases, Sibenik, Yugoslavia, 1984 (World Scientific, Singapore), p. 937.

Chen, F.F., 1987, Proceedings of the 1987 International Conference on Plasma Physics, Kiev, USSR, Vol. 4, p.321.

Chen, P., J.M. Dawson, R.W. Huff, and T. Katsouleas, 1985, Phys. Rev. Letters 54, 693.

Chen, P., 1986, Particle Accelerators 20, 171.

Chen, P., J.J. Su, J.M. Dawson, K.L.F. Bane, and P.B. Wilson, 1986, Phys. Rev. Letters 56, 1252.

Chen, P., J.J. Su, T. Katsouleas, S. Wilks, and J.M. Dawson, 1987, in: Katsouleas, 1987 (loc. cit.), p. 218.

Clayton, C.E., C. Joshi, C. Darrow, and D. Umstadter, 1985, Phys. Rev. Letters 54, 2343; 55, 1652.

Coffey, T.P., 1971, Phys. Fluids 14, 1402.

Cohen, B.I., A.N. Kaufman, and K.M. Watson, 1972, Phys. Rev. Letters 29, 581.

Dangor, A.E., A.K.L. Dymoke-Bradshaw, A. Dyson, T. Garvey, I. Mitchell, A.J. Cole, C.N. Danson, C.B. Edwards, and R.G. Evans, 1987, in: Katsouleas, 1987 (loc. cit.), p. 161 and in: Mills, 1987 (loc. cit.), p. 112.

Darrow, C., D. Umstadter, T. Katsouleas, W.B. Mori, C.E. Clayton, and C. Joshi, 1986, Phys. Rev. Lett. 56, 2629.

Darrow, C., W.B. Mori, T.Katsouleas, C. Joshi, D. Umstadter, and C.E. Clayton, 1987, in: Katsouleas, 1987 (loc. cit.), p. 107.

Dawson, J.M., 1959, Phys. Rev. 113, 383.

Dawson, J.M., V.K. Decyk, R.W. Huff, I. Jechart, T. Katsouleas, J.N. Leboeuf, B. Lembege, R.M. Martinez, Y. Ohsawa, and S.T. Ratliff, 1983, Phys. Rev. Lett. 50, 1455.

Fedele, R., U. deAngelis, and T. Katsouleas, 1986, Phys. Rev. A33, 4412.

Felber, F.S., 1980, Phys. Fluids 23, 1410.

Forslund, D.W., J.M. Kindel, W.B. Mori, C. Joshi, and J.M. Dawson, 1985, Phys. Rev. Letters 54, 558.

Fraser, J.S., 1987, in: Mills, 1987 (loc. cit.), p. 335.

Gribov, B.E., R.Z. Sagdeev, V.D. Shapiro, and V.I. Shevchenko, 1985, JETP Letters 42, 63.

Jackson, E.A., 1960, Phys. Fluids 3, 831.

Joshi, C., C.E. Clayton, and F.F. Chen, 1982, Phys. Rev. Letters 48, 874.

Joshi, C. and T. Katsouleas, eds., 1985, Laser Acceleration of Particles, Malibu, California, 1984 (Conference Proceedings No. 130, American Institute of Physics, New York).

Joshi, C., T. Katsouleas, C.E. Clayton, W.B. Mori, J.M. Kindel, and

D.W. Forslund, 1987a, in: Mills, 1987 (loc. cit.), p. 71.

Joshi, C., C.E. Clayton, K. Marsh, R. Williams, and W. Leemans, 1987b, in: Turner, 1987 (loc. cit.), p. 351.

Karttunen, S.J., and R.R.E. Salomaa, 1986, Phys. Rev. Letters 56, 604.

Karttunen, S.J., and R.R.E. Salomaa, 1987, in: Katsouleas, 1987 (loc. cit.), p. 134.

Katsouleas, T., and J.M. Dawson, 1983, Phys. Rev. Lett. 51, 392.

Katsouleas, T., 1984, University of California, Los Angeles, Report PPG-769.

Katsouleas, T., C. Joshi, J.M. Dawson, F.F. Chen, C.E. Clayton, W.B. Mori, C. Darrow, and D. Umstadter, 1985a, in: Joshi and Katsouleas, 1985 (loc. cit.), p. 63.

Katsouleas, T., J.M. Dawson, D. Sultana, and Y.T. Yan, 1985b, IEEE Trans. Nucl. Sci. NS-32, 3554.

Katsouleas, T. 1986, Phys. Rev. A33, 2056.

Katsouleas, T., ed., 1987, IEEE Transactions of Plasma Science, Vol. PS-15, April, 1987 (Institute of Electrical and Electronics Engineers, New York).

Katsouleas, T., and W. B. Mori , 1987, University of California, Los Angeles, Report PPG-1040.

Katsouleas, T., S. Wilks, P. Chen, J. M. Dawson, and J. J. Su, 1987a, Particle Accelerators 22, 81.

Katsouleas, T., J.M. Dawson, W.B. Mori, J.J. Su, and S. Wilks, 1987b, in: Turner, 1987 (loc. cit.), p. 401.

Kaw, P.K., A.T. Lin, and J.M. Dawson, 1973, Phys. Fluids 16, 1967.

Keinigs, R., and M.E. Jones, 1987, Phys. Fluids 30, 252.

Keinigs, R., M.E. Jones, and J.J. Su, 1987, in: Katsouleas, 1987 (loc. cit.), p. 199.

Kitagawa, Y. et al., 1987, in Turner, 1987 (loc. cit.), p. 386.

Koch, P., and J. Albritton, 1975, Phys. Rev. Letters 34, 1616.

Kruer, W.L. and E.M. Campbell, 1988, this volume.

Kuz'menkov, L.S., A.A. Sokolov, and O.O. Trubachev, 1983, Izv. Vyssh. Uchebn. Zaved. Fiz. 12, 17 [Sov. Phys. J. 26, 1076 (1984)].

Lee, P.S., Y.C. Lee, C.T. Chang, and D. S. Chuu, 1973, Phys. Rev. Letters 30, 538.

Martin, F., P. Brodeur, J.P. Matte, H. Pepin, and N. Ebrahim, 1987, in: Katsouleas, 1987 (loc. cit.), p. 167 and in: Mills, 1987 (loc. cit.), p. 121.

Max, C.E., J. Arons, and A.B. Langdon, 1974, Phys. Rev. Letters 33, 209.

McKinstrie, C.J., 1988, Phys. Fluids 31, 288.

McKinstrie, C.J., and D.W. Forslund, 1987, Phys. Fluids 30, 904.

McKinstrie, C.J., and D.F. DuBois, 1986, Phys. Rev. Letters 57, 2022 and 58, 286.

Mills, F.E., ed., 1987, Advanced Accelerator Concepts, Madison, Wisconsin, 1986 (Conference Proceedings No. 156), American Institute of Physics, New York).

Mima, K., and K. Nishikawa, 1984, Handbook of Plasma Physics (North Holland, Amsterdam), Vol. 2, p. 451.

Mima, K., T. Ohsuga, H. Takabe, K. Nishihara, T. Tajima, E. Zaidman, and W. Horton, 1986, Phys. Rev. Lett. 57, 1421.

Montague, B. W., and W. Schnell, 1985, in: Joshi and Katsouleas, 1985 (loc. cit.), p. 146.

Mori, W.B., 1987a, in: Katsouleas, 1987 (loc. cit.), p. 88.

Mori, W.B., 1987b, Thesis, University of California, Los Angeles.

Nishida, Y., M. Yoshizumi, and R. Sugihara, 1985, Phys. Fluids 28, 1574.

Nishida, Y., N. Sato, and T. Nagasawa, 1987, in: Katsouleas, 1987 (loc. cit.), p. 243.

Nishida, Y., and N. Sato, 1987, Phys. Rev. Lett. 59, 653.

Nishihara, N., 1975, J. Phys. Soc. Japan 39, 803.

Noble, R.J., 1985, Phys. Rev. A32, 460.

Pesme, D., S.J. Karttunen, R.R.E. Salomaa, G. Laval, and N. Silvestre, 1987, in Turner, 1987 (loc. cit.), p. 418.

Rosenbluth, M.N., and C.S. Liu, 1972, Phys. Rev. Letters 29, 701.

Rosenzweig, J.B., D.B. Cline, R.N. Dexter, D.J. Larson, A.W. Leonard, K.R. Mengelt, J.C. Sprott, F.E. Mills, and F.T. Cole, 1985, in: Joshi and Katsouleas, 1985 (loc. cit.), p. 226.

Rosenzweig, J., 1987, in: Katsouleas, 1987 (loc. cit.), p. 186; Phys. Rev.

Lett. 58, 555.

Rosenzweig, J., D. Cline, B. Cole, J. Detra, and P. Sealy, 1987, in: Mills, 1987 (loc. cit.), p. 231.

Ruth, R.D., A. Chao, P.L. Morton, and P.B. Wilson, 1985, Particle Accelerators 17, 171.

Sagdeev, R.Z. and V.D. Shapiro, 1973, JETP Letters 17, 279.

Sakai, K., S. Takeuchi, and M. Matsumoto, 1984, Inst. of Plasma Physics, Nagoya, Japan Report IPPJ-680.

Schmidt, G., and W. Horton, 1985, Comments on Plasma Phys. 9, 85.

Singer, S., 1985, in: Joshi and Katsouleas, 1985 (loc. cit.), p. 475.

Sprangle, P., C.M. Tang, and E. Esarey, 1987, in: Katsouleas, 1987 (loc. cit.), p. 145.

Stansfield, B.L., R. Nodwell, and J. Meyer. 1971, Phys. Rev. Letters 26, 1219.

Su, J.J., T. Katsouleas, J.M. Dawson, P. Chen, M. Jones, and R. Keinigs, 1987, in: Katsouleas, 1987 (loc. cit.), p. 192.

Sugihara, R., S. Takeuchi, K. Sakai, and M. Masumoto, 1984, Phys. Rev. Lett. 52, 1500.

Sullivan, D.J., and B.B. Godfrey, 1983, in: Channel, P.J., 1983 (loc. cit.), p. 3244.

Tajima, T., and J.M. Dawson, 1979, Phys. Rev. Lett. 43, 267.

Tang, C.M., P. Sprangle, and R.N. Sudan, 1985, Phys. Fluids 28, 1974.

Turner, S., ed., 1987, Workshop on New Developments in Particle Acceleration Techniques, Orsay, France 1987 (CERN Report No. 87-11 or Report No. 87/110, European Committee for Future Accelerators).

Umstadter, D., R. Williams, C. Clayton, and C. Joshi, 1987, Phys. Rev. Lett. 59, 292.

Umstadter, D.P., 1987, Thesis, University of California, Los Angeles.

Wilks, S., T. Katsouleas, J.M. Dawson, P. Chen, and J.J. Su, 1987, in: Katsouleas, 1987 (loc. cit.), p. 210.

Figure Legends

1. Conceptual scheme of a Beat-wave Accelerator module.

2. Injection and acceleration of electrons in the BWA. (a) A short pulse of laser light, imbedded with synchronized electron bunches, travels through non-resonant plasma. (b) As the light pulse and the bunches enter the region of resonant density synchronously, an EPW grows around the electrons. Sufficiently energetic electrons are trapped in alternate half-cycles of the EPW as the potential barrier grows up behind them. (c) Behind the light pulse, the EPW is de-excited as its relativistic frequency shift causes a phase mismatch with the beat pattern. The electrons also slip in phase as they gain velocity.

3. Schematic diagram of fields in a two-dimensional plasma wave. (a) Isopotential contours; (b) longitudinal E-field, with accelerating region (for e^+) shown enhanced; (c) transverse E-field, with focusing region (for e^+) shown enhanced; (d) wave potential, with region of both acceleration and focusing shown enhanced.

4. Two-dimensional simulation of test particle trapping and acceleration in the BWA. Laser beams of width $30c/\omega_p$ with a $\cos^2$ y profile are incident from the left, and test particles are uniformly injected in x-y phase space. The trapping of bunches at the appropriate EPW phase is seen at $T = 180\ \omega_p^{-1}$. At later times, planarity is lost because EPW saturation depends on radius. (Joshi et al., 1987a).

5. Experimental arrangement of Clayton et al. (1985) and (inset) signature of beat wave detected by Thomson scattering.

6. Physical mechanism of the Plasma Wake-field Accelerator: (a) equipotentials and E-vectors in the plasma-wave wake following a driving bunch; (b)

density profiles for optimized driving and driven bunches; (c) longitudinal E-field in various regions. For clarity, electrons are taken to be positive.

7. Wake of a one-dimensional charge in the beam frame.

8. One-dimensional computer simulation of an ideal driving pulse, showing both the wake field and the retarding field within the pulse, for the case R = 7.1. (P. Chen et al., 1986.)

9. One-dimensional simulation of a wake field loaded with an ideal triangular bunch with 75% efficiency. In (a) the bunch is located where the wake is flat-topped. In (b) is shown the energy gain at $\omega_p t = 40$ of particles within the bunch. (From Wilks et al., 1987.)

10. Amplitudes of the harmonics n_2/n_o and n_3/n_o at $2\omega_p$, $2k_p$ and $3\omega_p$, $3k_p$, as functions of the fundamental amplitude n_1/n_o, measured experimentally by Umstadter et al. (1987). The lines are theoretical predictions, and the dashed limits reflect the error bars on n_1/n_o.

11. Temporal behavior of mode coupling due to an ion ripple. (a) Beat wave and first four coupled modes in an 8% ripple. (b) Beat wave saturation with increasing ripple amplitude. (From Darrow et al., 1986).

12. Electrostatic modes observed by Thomson scattering in the beat-wave experiment of Darrow et al. (1986). The desired beat wave is at (ω_p, k_p). Open circles indicate scattering from ion waves and their harmonics. Modes at $(\omega_p, k_p \pm mk_i)$ are due to mode coupling. Modes at $(2\omega_p, mk_i)$ are mode coupled from plasma wave harmonics.

13. (a) Geometry of the surfatron accelerator. (b) Particle trajectory in $v_x - v_y$ phase space, showing damping of oscillations and surfing angle θ.

14. Mechanism of the plasma lens. A cylindrical electron bunch with density profile shown by the dashed lines moves through a plasma. The plasma electrons $\ominus$ are pushed outwards by the head of the beam, leaving an excess ion $\boxplus$ charge which attracts electrons in the tail of the beam toward the axis. For positron beams, the electron motion is reversed, but the effect is the same. (P. Chen et al., 1987).

15. Simulation of the focusing effect of a thick lens. The precursor electrons are not focused. (P. Chen et al., 1987).

16. Schematic of a converging plasma wave accelerator. (F. Chen, 1985).

TABLE 1

Instabilities in Plasma Accelerators

Energy source	Electrons only	Ion motions also
Laser radiation	SRS modified SRS Compton scattering forward scattering relativistic self-modulation self-focusing filamentation	SBS modified SBS Compton scattering ponderomotive self-modulation self-focusing filamentation
Plasma wave	modulational instability (relativistic) resonant self-focusing (relativistic)	modulational instability (ponderomotive) resonant self-focusing (ponderomotive)
Particle beams	two-stream filamentation (Weibel) self-focusing (pinch) sausage and firehose	ion-acoustic (Buneman)

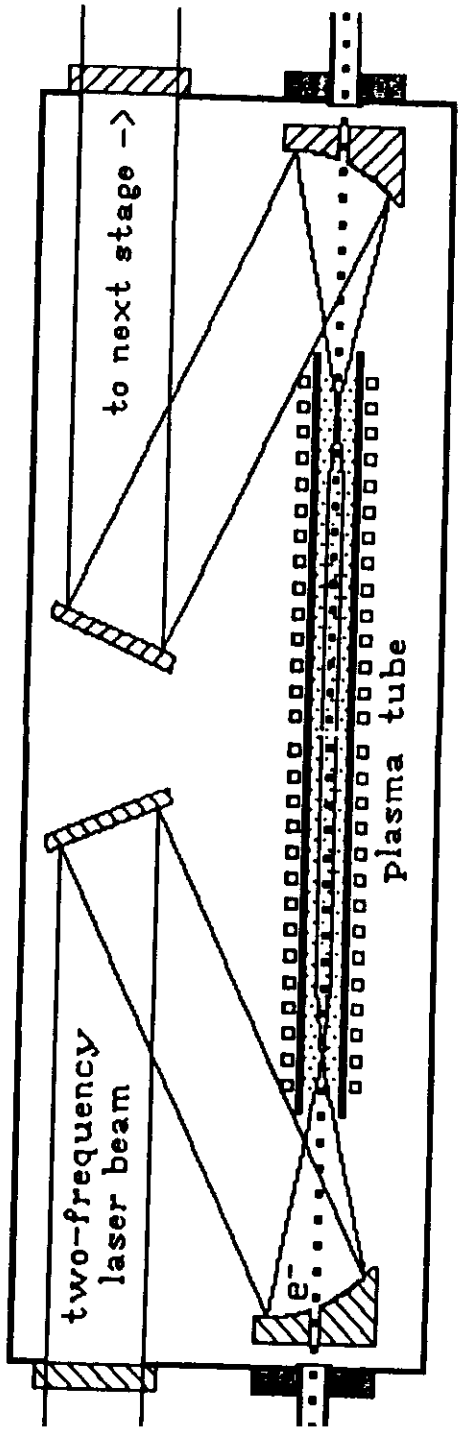

Figure 1

Note: Subsequent figures should be numbered n+1.

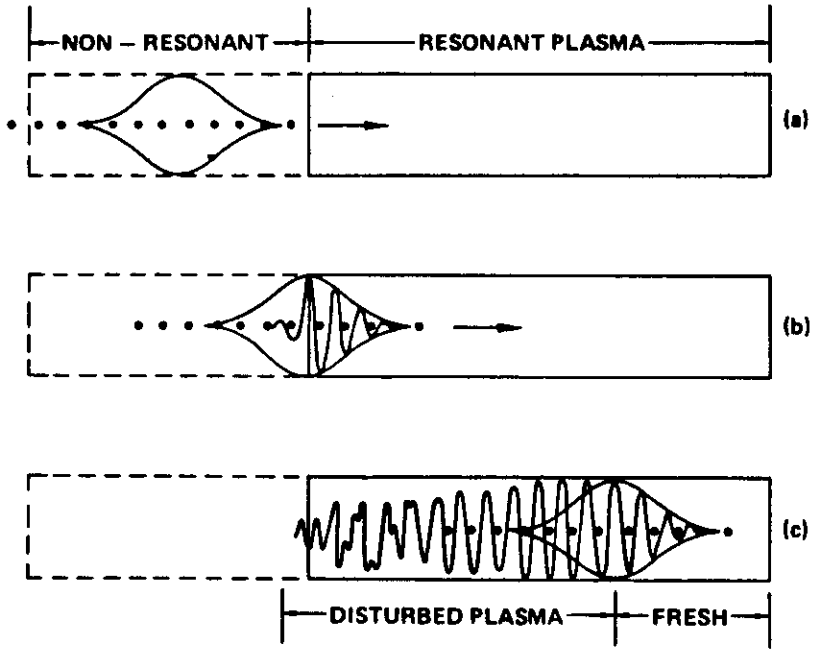

Fig. 1. Injection and acceleration of electrons in the BWA. (a) A short pulse of laser light, imbedded with synchronized electron bunches, travels through non-resonant plasma. (b) As the light pulse enters region of resonant density, it excites an EPW. Sufficiently energetic electrons pass over the evanescent wave region and are trapped in alternate half-cycles of the EPW. (c) Behind the light pulse, the EPW is de-excited as its relativistic frequency shift causes a phase mismatch with the beat pattern. The electrons also slip in phase as they gain velocity.

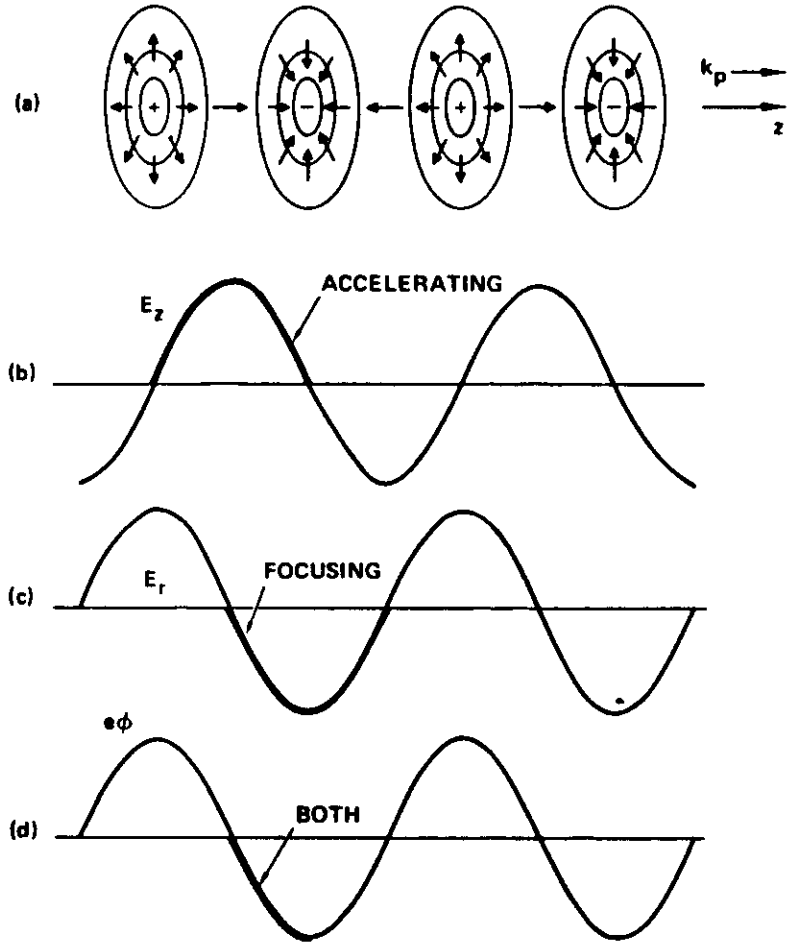

Fig. 2. Schematic diagram of fields in a two-dimensional plasma wave. (a) Isopotential contours; (b) longitudinal E-field, with accelerating region (for e^+) shown enhanced; (c) transverse E-field, with focusing region (for e^+) shown enhanced; (d) wave potential, with region of both acceleration and focusing shown enhanced.

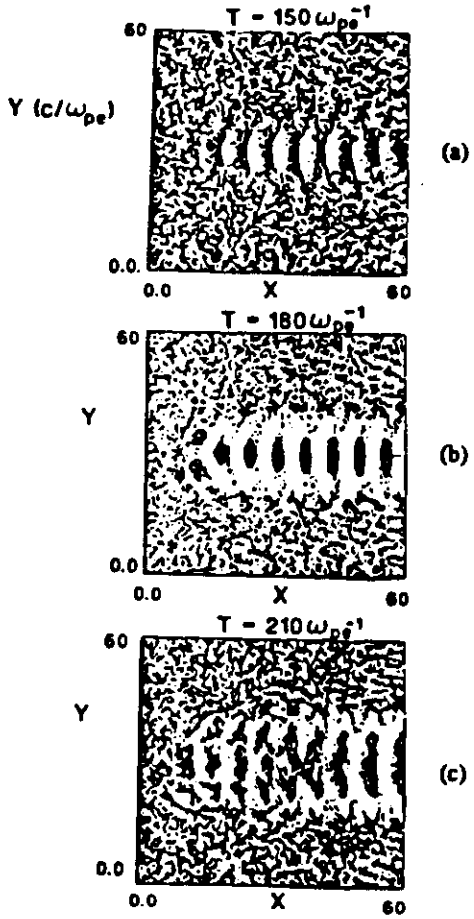

Fig. 3. Two-dimensional simulation of test particle trapping and acceleration in the BWA. Laser beams of width $30c/\omega_p$ with a $\cos^2$ y profile are incident from the left, and test particles are uniformly injected in x-y phase space. The trapping of bunches at the appropriate EPW phase is seen at $T = 180\ \omega_p^{-1}$. At later times, coherence is lost because EPW saturation depends on radius. (Joshi et al., 1987).

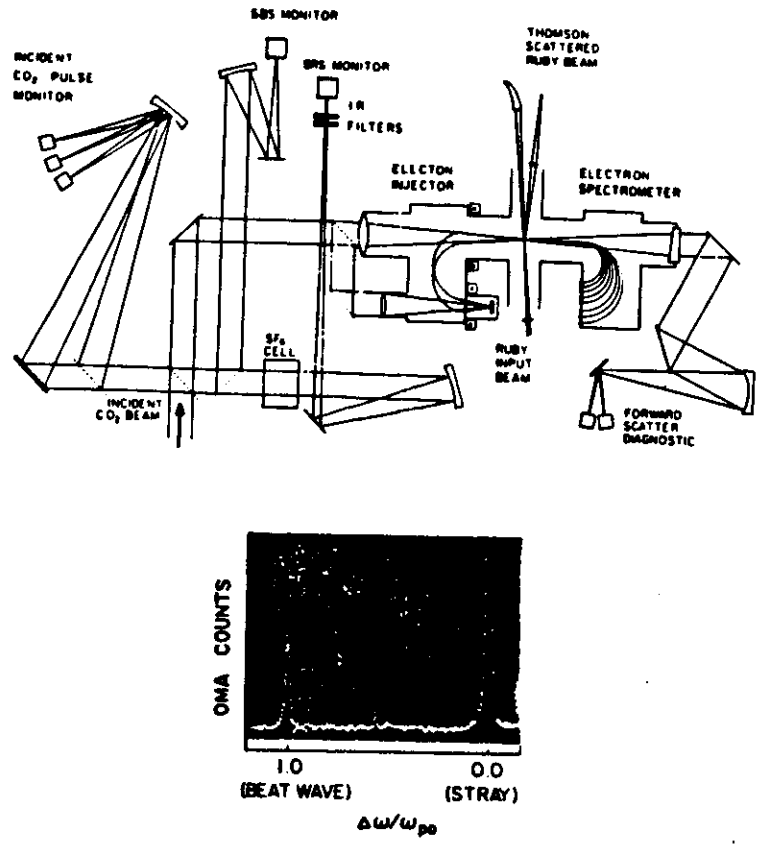

Fig. 4. Experimental arrangement of Clayton et al. (1985) and (inset) signature of beat wave detected by Thomson scattering.

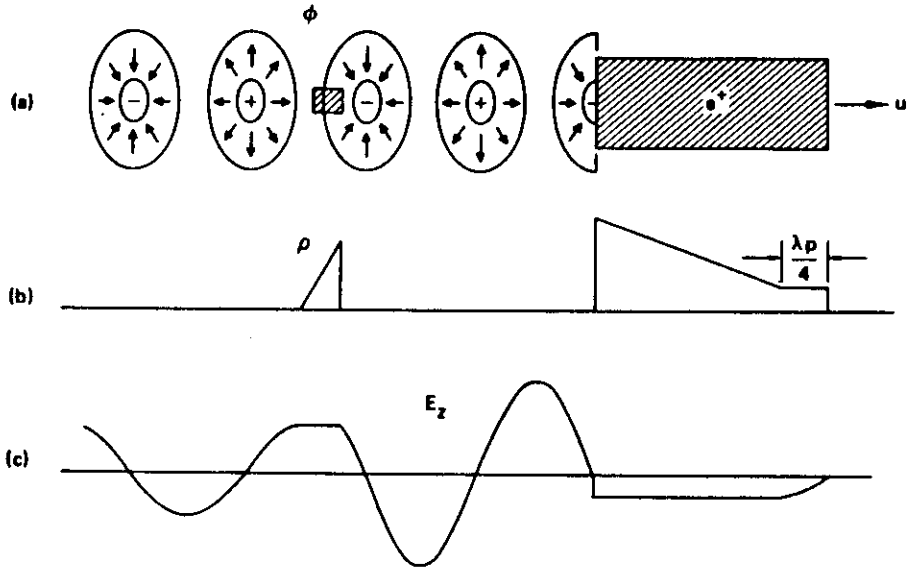

Fig. 5. Physical mechanism of the Plasma Wake-field Accelerator: (a) equipotentials and E-vectors in the plasma-wave wake following a driving bunch; (b) density profiles for optimized driving and driven bunches; (c) longitudinal E-field in various regions. For clarity, electrons are taken to be positive.

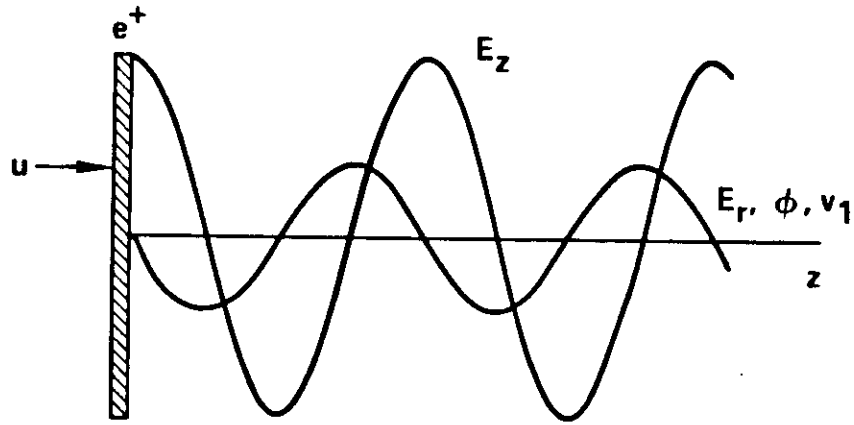

Fig. 6. Wake of a one-dimensional charge in the beam frame.

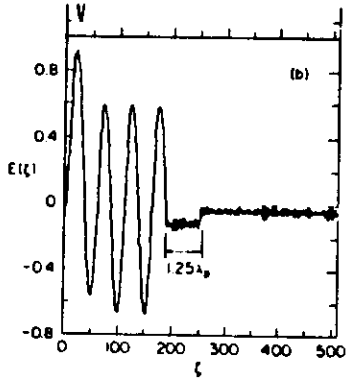

Fig. 7. One-dimensional computer simulation of an ideal driving pulse, showing both the wake field and the retarding field within the pulse, for the case R = 7.1. (P. Chen et al., 1986.)

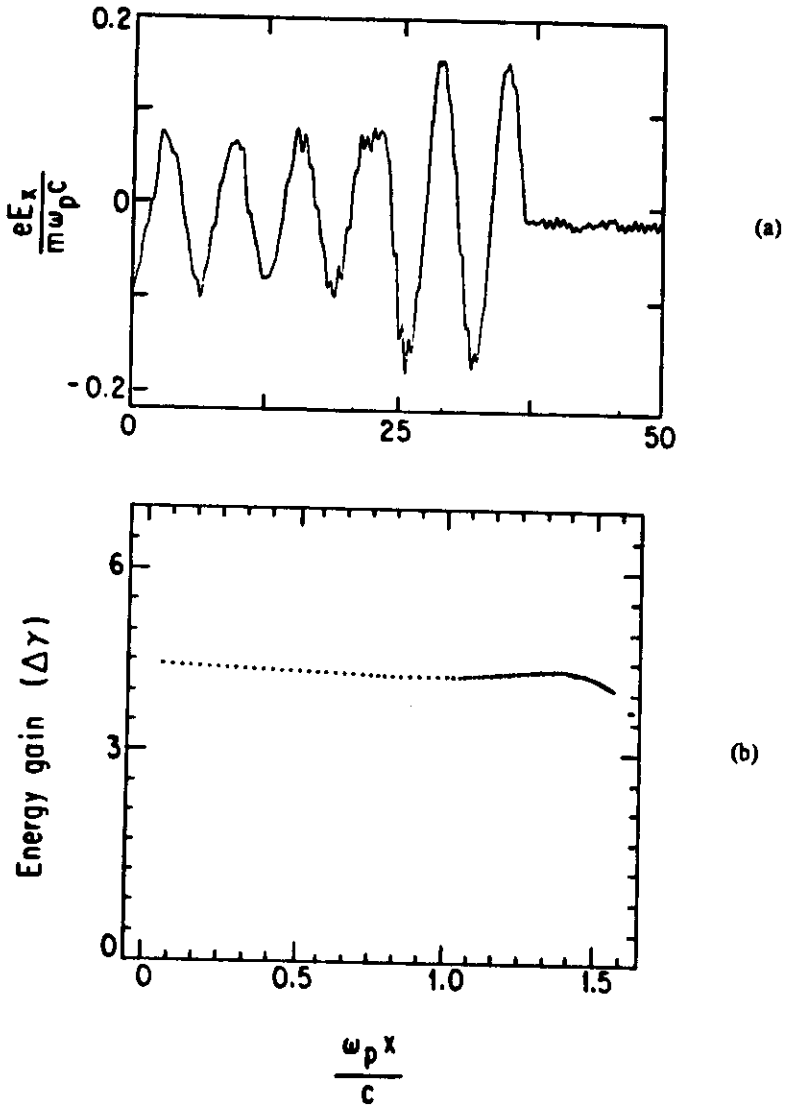

Fig. 8. One-dimensional simulation of a wake field loaded with an ideal triangular bunch with 75% efficiency. In (a) the bunch is located where the wake is flat-topped. In (b) is shown the energy gain at $\omega_p t = 40$ of particles within the bunch. (From Wilks et al., 1987.)

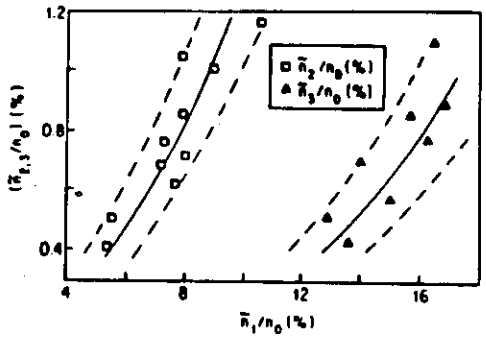

Fig. 9. Amplitudes of the harmonics n_2/n_0 and n_3/n_0 at $2\omega_p$, $2k_p$ and $3\omega_p$, $3k_p$, as functions of the fundamental amplitude n_1/n_0, measured experimentally by Umstadter et al. (1987). The lines are theoretical predictions, and the dashed limits reflect the error bars on n_1/n_0.

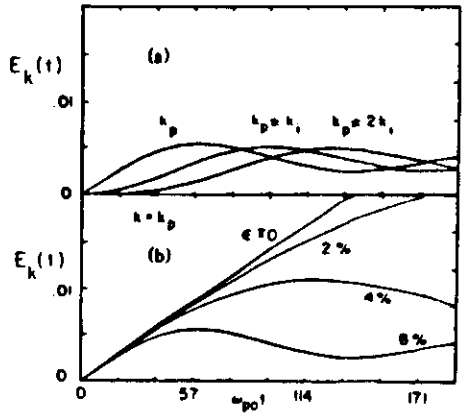

Fig. 10. Temporal behavior of mode coupling due to an ion ripple. (a) Beat wave and first four coupled modes in an 8% ripple. (b) Beat wave saturation with increasing ripple amplitude. (From Darrow et al., 1986).

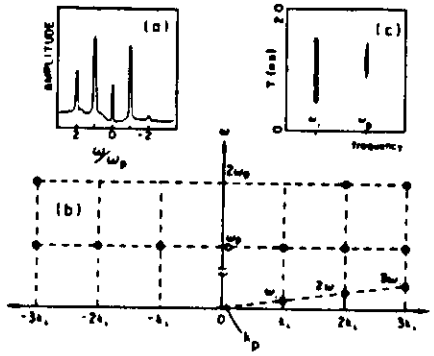

Fig. 11. Electrostatic modes observed by Thomson scattering in the beat-wave experiment of Darrow et al. (1986). The desired beat wave is at (ω_p, k_p). Open circles indicate scattering from ion waves and their harmonics. Modes at $(\omega_p, k_p \pm mk_i)$ are due to mode coupling. Modes at $(2\omega_p, mk_i)$ are mode coupled from plasma wave harmonics.

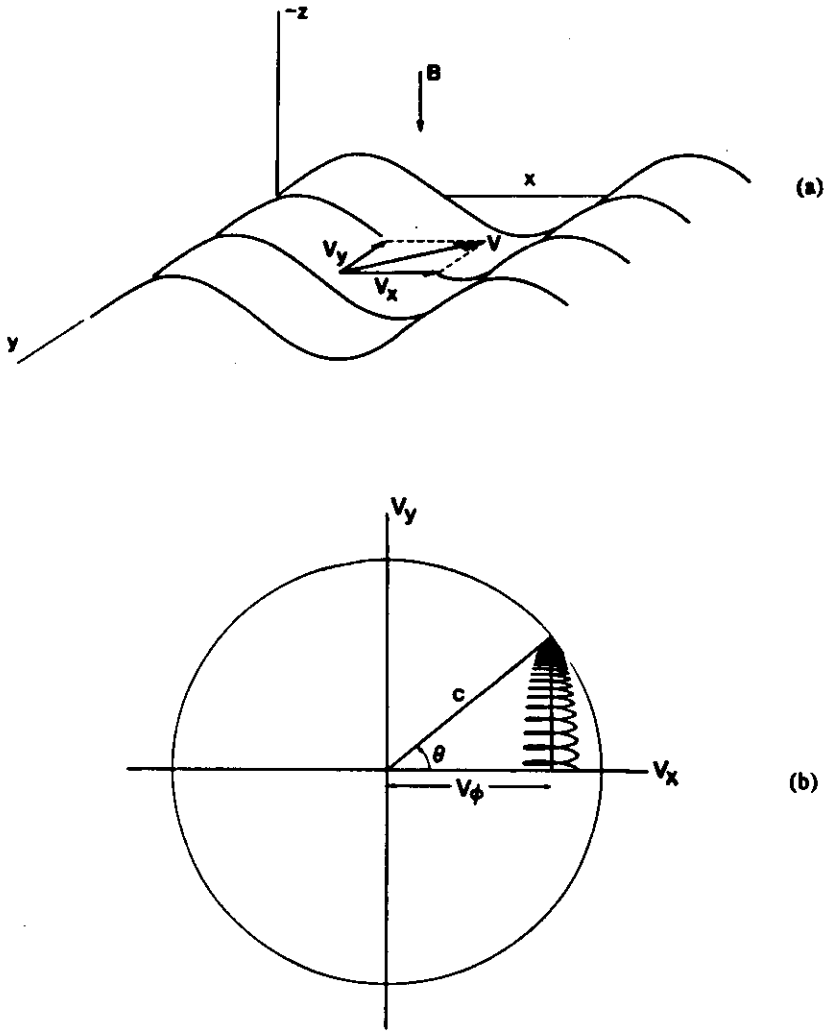

Fig. 12. (a) Geometry of the surfatron accelerator. (b) Particle trajectory in $v_x - v_y$ phase space, showing damping of oscillations and surfing angle θ.

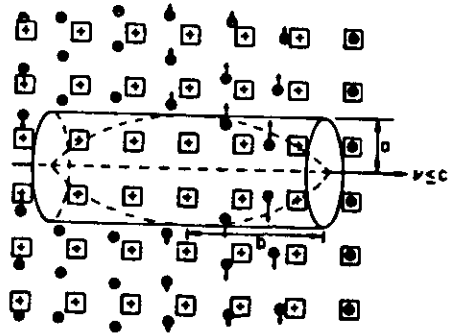

Fig. 13. Mechanism of the plasma lens. A cylindrical electron bunch with density profile shown by the dashed lines moves through a plasma. The plasma electrons ⊖ are pushed outwards by the head of the beam, leaving an excess ion ⊕ charge which attracts electrons in the tail of the beam toward the axis. For positron beams, the electron motion is reversed, but the effect is the same. (P. Chen, 1986).

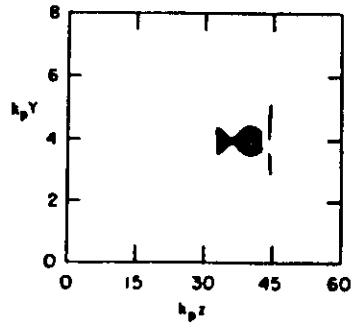

Fig. 14. Simulation of the focusing effect of a thick lens. The precursor electrons are not focused. (P. Chen, 1986).

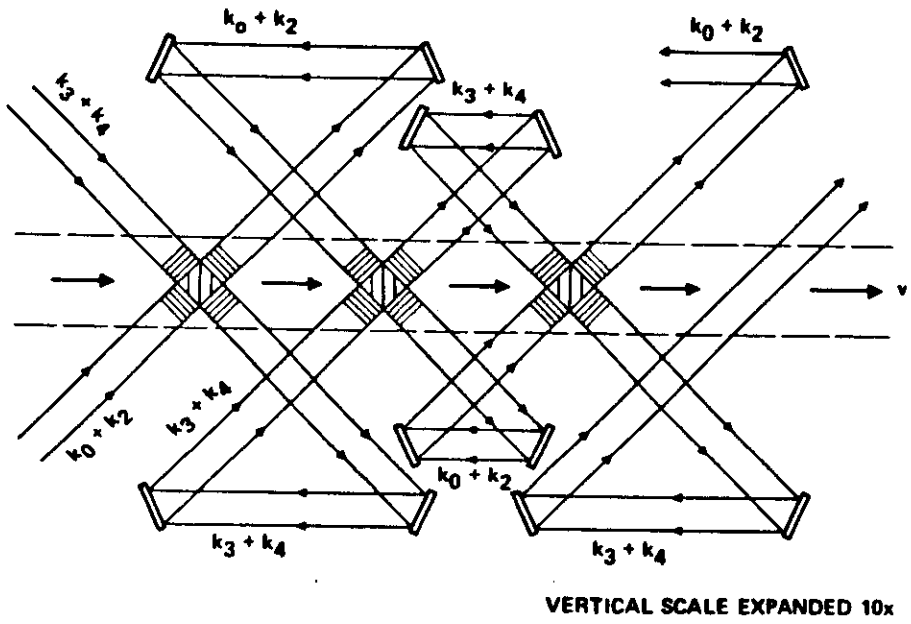

Fig. 15. Schematic of a converging plasma wave accelerator. (F. Chen, 1985).